JPRS-UPM-92-002
16 MARCH 1992

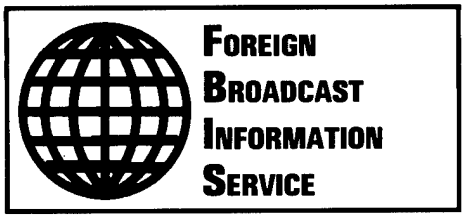

JPRS Report

Science & Technology

Central Eurasia: Physics & Mathematics

Science & Technology
USSR: Physics & Mathematics

JPRS-UPM-92-002 *16 March 1992*

CONTENTS

ACOUSTICS

CRYSTALS, LASER GLASSES, SEMICONDUCTORS

FLUID DYNAMICS

LASERS

NUCLEAR PHYSICS

OPTICS, SPECTROSCOPY

PLASMA PHYSICS

SUPERCONDUCTIVITY

TECHNICAL PHYSICS

THERMODYNAMICS

THEORETICAL PHYSICS

DIFFERENTIAL EQUATIONS

Explosive Accelerator of Tungsten Powder Particles in Cylindrical Cup

927J0048B Minsk INZHENERNO-FIZICHESKIY ZHURNAL in Russian Vol 61 No 1, Jul 91, pp 46-51

[Article by S. K. Andilevko, G. S. Romanov, and S. M. Usherenko, Belorussian Republic's Scientific-Industrial Association for Powder Metallurgy, Minsk]

UDC 534.2

[Abstract] An accelerator of tungsten powder particles for blast treatment of hard surfaces is considered which consists of a solid explosive charge formed into a circular cylindrical cup holding the powder, with a center hole behind the powder for an electrical detonator rod and with a guide sleeve for the powder jet which extends beyond the rim. For computer-aided design and performance analysis of this device, it is assumed to be symmetric about both its longitudinal z-axis and radial r-axes. It is discretized into a uniform space grid of fictitious cells with $h_r = h_z$ sides each and the explosion process is discretized in time by averaging the velocity over three successive cells. The boundary conditions are: 1) impermeability along the z-axis (r = 0) and of the lateral inside surfaces so that the radial velocity of the powder jet reverses direction while all other quantities do not change; 2) discharge into vacuum at both back (z = 0) and front (z = 1) surfaces. The equation of energy for the propagating detonation wave and Tate's equation of state for pressure of the tungsten powder have been solved numerically on this grid, the results indicating that acceleration of the powder jet is characterized by an approximately exponential increase of its velocity. They have also been solved for an accelerator without a focusing guide sleeve, the results revealing the advantages and effectiveness of the latter. Figures 6; references 9.

Sensitivity and Speed of Superconducting Optoelectronic Heat Detector

927J0048C Minsk INZHENERNO-FIZICHESKIY ZHURNAL in Russian Vol 61 No 1, Jul 91 pp 136-140

[Article by O. S. Yesikov, A. I. Krot, Ye. A. Protasov, V. P. Sobolev, and V. S. Kharitonov, Moscow Institute of Engineering Physics]

UDC 535.231.62:621.315.5:538.945

[Abstract] A new optoelectronic heat detector with a sensor consisting of a Y-Ba-Cu-O superconductor film on a $SrTiO_3$ substrate layer is considered, its performance under uniform irradiation of its active surface being analyzed for response speed and sensitivity. Inasmuch as the superconducting film is much thinner than the substrate layer and the thermophysical properties of the two materials are not very different, one may assume that the behavior of such a sensor is determined only by the thermophysical properties of the substrate material and the thermal resistance of the film. A sensor in the form of a circular superconductor film on a circular substrate is considered, this structure being mounted symmetrically on a thermostat ring (short and thick hollow cylinder) with a thin regulator film between them. The substrate is continuously cooled with liquid nitrogen fed into that center hole of the thermostat. Evolution of the temperature profiles T(z,t) across the sensor film thickness during downward heat transfer and T(r,t) across the sensor film surface during lateral heat transfer, upon downward incidence of thermal radiation, is described by the general expression $T_{t\to\infty}(x) - (T_{max} - T_{stat})\Sigma_{n=1}^{\infty}A_n \cos(\mu_n x/L)\exp(-\mu_n^2 at/L^2)$ (x = z,r; $T_{t\to\infty}$ is the steady-state substrate temperature profile, T_{max} - maximum sensor temperature, T_{stat} - thermostat temperature $\approx$ 77 K, L - thickness d of substrate or radius R of sensor film, a - thermal diffusivity same of both materials, coefficients A_n and μ_n depending on the ratio of thermal resistance P_{sub} of substrate to thermal resistance P_{reg} of regulator film). The temperature sensitivity S_T, quotient of change of sensor (superconductor film) temperature divided by density of incident thermal flux, is in the case of downward heat transfer equal to the quotient d/λ of substrate thickness divided by thermal conductivity of the substrate material plus the product $P_{reg}F$ of thermal resistance of the regulator film multiplied by the sensor film surface area F. In the case of lateral heat transfer the quotient is $P^2/2d\lambda$ and must be multiplied by the factor $1 - r^2/R^2$. The response speed of the sensor, which characterizes its thermal inertia, is defined as the time taken for the sensor temperature to rise to half its maximum level $t_{1/2} \approx B\rho c_p V(4R_{sub} + \pi^2 R_{reg})/\pi^2$ (ρ - density of substrate material, c_p - specific heat at constant pressure, V - volume of substrate, coefficient B depending on the ratio P_{sub}/P_{reg} of thermal resistances and being a function of the z-coordinate in the case of downward heat transfer or a function of the r-coordinate in the case of lateral heat transfer). Thermal sensitivity and response speed can be combined into a single sensor performance indicator $S_T/t_{1/2} \approx 1/BC_{sub}$ (C_{sub} - heat capacity of substrate). In an experiment with a 1 μm thick and 6.8 mm in diameter Y-Ba-Cu-O sensor film (density 6.35 g/cm^3, thermal conductivity 2.8 W/m.K, specific heat 105-205 J/kg.K) on a 0.3 mm thick and 9.0 mm in diameter $SrTiO_3$ substrate (density 6.45 g/cm^3, thermal conductivity 4.5 W/m.K, specific heat 165 J/kg.K) the center hole of the thermostat was 5.0 mm in diameter and thermal resistance of the regulator film was varied over the 2-2500 W/K range. A sensitivity of almost 0.05 K.m^2/W (1,400 K/W) and a speed of about 1.5 s were obtained with a 2500 W/K thermal resistance of the regulator film. Figures 3; references 8.

Analysis of Acoustooptical Conversion in Nematic Liquid Crystals

927J0049A Moscow AKUSTICHESKIY ZHURNAL in Russian Vol 37 No 3, May-Jun 91 pp 497-504

[Article by O. A. Kapustina and V. N. Reshetov, Institute of Acoustics imeni N. N. Andreyev, USSR Academy of Sciences]

UDC 534:535

[Abstract] The acoustooptical conversion in a nematic liquid crystal resulting in polarization modulation of incident light, namely reorientation of crystal molecules in an oscillating hydrodynamic flux of nematic liquid according to the P(t) (alternating pressure in incident acoustic wave) → V(t) (oscillating hydrodynamic flux of nematic liquid) → φ(z,t) (angle which characterizes reorientation of crystal molecules) → Φ(t) (phase difference between ordinary "o" and extraordinary "e" light rays) → I(t) (intensity of light), is analyzed on the basis of equations completely describing the behavior of such a crystal (viscous and anisotropic incompressible fluid) in an acoustic field. These are the Navier-Stokes equation for the three orthogonal $V_{x,y,z}$ velocity components, the continuity equation, and the equation of motion for the director n[1]. Linearization of this system of equations, permissible when the intensity of the acoustic field is sufficiently moderate for effecting an only $\varphi(t) << 1$ rad reorientation of molecules, reduces it to one which describes flow of a nematic liquid crystal in a flat capillary and deflection of the director from the Z-axis in the velocity field. As a specific case is considered a quasi-homeomorphic orientation of molecules ($\varphi_0 << 1$) in a hydrodynamic flux which oscillates in the XOY plane predominantly along the Y-axis so that $V_y >> V_{x,z}$ and a velocity field which varies "fast" along that Y-axis while remaining quasi-constant along both other (X,Z) axes. The correspondingly modified system of equations splits into independent equations for crystals whose thickness is much smaller than length of the viscosity wave and much larger than length of the orientation wave, which corresponds to frequencies much smaller than ω_B and much larger than ω_H. The solution to these equations describes the initial stages of acoustooptical conversion, namely the V(P) dependence and φ(V) dependence, including the profile of dynamic reorientation across the layer of a nematic liquid crystal in a flat capillary. The later stages of acoustooptical conversion in such a layer, including the Φ(φ) dependence of the phase difference between ordinary and extraordinary light rays on the director oscillation angle, are described by a modification of the classical Born-Wolf equation of crystal optics which takes into account orientation profile of molecules across the thickness of such a layer. On this basis is then obtained an expression for the intensity of light after passage successively through a nematic liquid crystal and an analyzer. An expression finally obtained for the coefficient of acoustooptical conversion by a sensor with a flat capillary containing a nematic liquid crystal and operating in the quasi-linear mode indicates that conversion efficiency is maximized by use of a thick (large d/L ratio) low-viscosity nematic liquid crystal with a large difference of refractive indices $\Delta n = n_e - n_o$ and operating in the quasi-linear mode with a high-order Φ_m phase difference harmonic. Tests were performed with a flat capillary containing a nematic liquid crystal as sensor and terminating at one of its two free ends into a horn, an either 150 μm thick aluminum or 15 μm thick beryllium membrane covering the horn aperture and thus insulating the crystal from the ambient medium while also "compensating" the amplitude-frequency characteristic of I(t) to P(t) sensor response. In these tests the acoustic impedance was varied from Z_0 (capillary alone) to $Z = Z_0 + Z_M$ (capillary + membrane). Tests were also performed inside a closed sound chamber, without a membrane. In these tests the acoustic impedance was varied from Z_0 (capillary alone to $Z_0 + Z_V$ (capillary + chamber) and the frequency of sound was varied so that its wavelength remained much smaller than the chamber dimensions, the upper limit of the frequency range (1 kHz) being lower than the first critical frequency for the chamber. Figures 3; references 7.

Nonlinear Sound Beam in Tube With Rigid Walls. Time-Average Field Parameters and Hydrodynamic Force

927J0049B Moscow AKUSTICHESKIY ZHURNAL in Russian Vol 37 No 3, May-Jun 91 pp 512-517

[Article by S. N. Makarov, Leningrad State University]

UDC 534.222

[Abstract] A sound beam passing from a radiator with an arbitrary amplitude distribution through a circular tube with impermeable rigid walls containing a barotropic fluid is considered, a sound beam of an intermediate form between the two extreme forms of a plane wave (tube with frictionless walls and diameter not larger than diameter of radiator) and a bounded beam in free space (tube diameter infinitely large and radiator parameters fixed). Determination of the time-average excess acoustic pressure and the hydrodynamic force is based on asymptotic expansions in the theory of nonlinear acoustic traveling waves involving not only the fundamental mode but also admitting new modes. The barotropic fluid is described by Tate's equation of state and only pressure waves are considered (solenoidal and thus hydrodynamic flow either not yet having developed or being still so weak that it can be disregarded), with the wave amplitude as the small parameter μ. All vibration parameters such as axial x-component v and radial r-component w of the vibration velocity as well as the excess pressure p' are assumed to be periodic functions of the "traveling" time $\tau = t - x/c$ (c - speed of sound) in μ-terms of both first and second orders of smallness without constant components in μ-terms of the first-order of smallness so that v[dash over v] = $0(\mu^2)$, w[dash over w] = $0(\mu^{2\ 1/2})$, ..., but aperiodicity appearing in μ-terms of the third-order of smallness $0(\mu^3)$ for v,p' and $0(\mu^{3\ 1/2})$ for w. The asymptotic corrections such as the amplitude of the reflected pressure wave $p_s = 0(\mu^3)$ is not, in the first-order approximation, a function of the "fast" time τ. This pressure p_s and the average excess pressure p[dash over p]' are, moreover, shown not to be functions of the radial coordinate r. It is furthermore proved that the method of a slowly varying profile will yield a system of equations in the third-order approximation for a

sound beam in a tube as well as one for the Earnshaw problem of an initially plane wave in a tube with a diameter smaller than that of the radiator. The hydrodynamic force F which induces a steady vortical flow through the tube is calculated by necessarily including its potential component, inasmuch as the gradient of acoustic pressure in a nonuniform acoustic field such as that in a tube can induce an attendant directional flow (it vanishes in free space). This component does not influence the flow velocity when the gradient of acoustic pressure is exactly balanced by the gradient of hydrostatic pressure and pressure thus does not appear explicitly in the boundary conditions, but does influence it otherwise as in the case of a vertical tube joining two constant-pressure sources. A horizontal tube with a radiator at one end can be regarded as an acoustic pump with a zero volume flow rate rather than with a volume flow rate not lower than around the sound beam axis in free space (according to V. Nieborg), a near zero volume flow rate in such a tube having been recorded in an experiment. The author thanks N. G. Semenova for helpful discussion. References 14.

Theory of Spatiotemporal Diffraction Tomography With Planar Scan by Single Transceiver

927J0049C Moscow AKUSTICHESKIY ZHURNAL in Russian Vol 37 No 3, May-Jun 91 pp 528-534

[Article by A. V. Osetrov, Leningrad Institute of Electrical Engineering imeni V. I. Ulyanov (Lenin)]

UDC 534.8

[Abstract] A method of acoustic spatiotemporal diffraction tomograghy for nondestructive inspection and medical diagnosis of objects is proposed which, by involving a planar scan with a single transceiver, combines high longitudinal space resolution of B-scan and high transverse space resolution of single-frequency holography. Reconstruction of an object's image is effected by transmission of a short pulse signal to the given plane and measurement of the signal reflected by each inhomogeneity as a function of time as well as a function of space coordinates x,y. In the scalar case the resultant (incident + scattered) field of each spectral component of both emitted and scattered signals within a region free primary sound sources is described by the differential equation $\Delta P(r,r',k) + k^2P(r,r', k) = G(r',k)$ (r - radial coordinate of transceiver location, r' - radial coordinate of given point within region of inhomogeneity, wave number $k = \omega/c_0$, ω - frequency of sound wave, c_0 - speed of sound in absence of inhomogeneities, P(r,r',k) - complex amplitude of acoustic field and specifically of acoustic pressure when in water or similar liquid, G(r',k) - function of inhomogeneities. The two most typical kinds of inhomogeneities are considered: 1) speed-of-sound inhomogeneities so that $G(r,k) = k^2[(c^2(r) - c_0^2/c^2(r)]$, 2) solid particles and gas bubbles with boundary conditions of either first or second kind so that $G(r,k) = +/-\Delta\gamma(r)$ (γ - characteristic function equal to 1 inside scatterer and to 0 outside a scatterer, $\Delta\gamma = 0$ at scatterer surface only). With the G(r,k) function expressed in the general form $G(r,k) = f(k)0(r)$, where $f(k) = k^2$ in the first case or f(k) in the second case and 0(r) is the sought function of inhomogeneities or of the object's image, that differential equation becomes one nonlinear with respect to 0(r). In the first-order Born approximation it reduces to $\Delta P_S(r,r',k) + k^2P_S(r,r',k) = f(k)0(r)P_I(r,r',k)$ ($P_S = P - P_I$, P_I - complex amplitude of incident acoustic field). In the case of a point transceiver $P_I(r,r',k) = A_0(k)e^{(ik|r-r'|)/(|r-r'|)}$ (A_0 - complex amplitude at unit distance from radiator at frequency $\omega = kc_0$). This approximation is valid for inhomogeneities of the first kind, where $|P_S| << |P_I|$. This approximation is not valid for inhomogeneities of the second kind and particularly for perfectly rigid or perfectly soft scatterers, which do not satisfy the relation $P_I >> P_S$ at their surface, also not in the shadow region. It may be applied also in the case of strong scatterers, however, when the meaning of function 0(r) is stipulated in accordance with Kirchhoff's equation for a field scattered by the closed surface of a scatterer so that P_S = surface integral of $(G_0\Delta P - P\Delta G_0)ds$ (G_0 - Green's function) or, upon introduction of the parameter $\mu = P|_S/P_I|_S$, P_S = volume integral of $0G_0P_I)dr$ ($0 = \mu(\delta/\delta n)(\delta_S)$, $(\delta/\delta n)(\delta_S$ - double layer of unit density on surface S, $\mu = 2$ in sounded region and $\mu = 0$ in shadow region). As a special case is considered simultaneous presence of density and compressibility perturbations. Figures 2; references 15.

Normal Transverse Impact With Friction by Rectangular Bar on Thread

927J0053B Moscow IZVESTIYA AKADEMII NAUK SSSR: MEKHANIKA TVERDOGO TELA No 3, May-Jun 91 pp 160-163

[Article by M. Ergashov, Tashkent]

UDC 624.07:534.1

[Abstract] Normal transverse impact with friction at time $t = 0$ on an infinitely long horizontal initially straight and flexible thread by a rectangular bar moving vertically down with a constant velocity at time $t \leq 0$ is analyzed, assuming that the bar surfaces are perfectly smooth and that pressure on the thread and friction are localized within infinitesimally small regions about the two incident bar edges. Such an impact generates four longitudinal and two transverse waves in the thread, with two stationary discontinuities: one at each bar edge. The problem is formulated as a two-dimensional one symmetric with respect to the center point of the thread segment under the bar, the behavior of the thread under appropriate dynamic and kinematic constraints being described by a system of five equations. Two equations $ds_3/(1 + \varepsilon_3) = ds_2/(1 + \varepsilon_1$ and $\rho_3(1 + \varepsilon_3) = \rho_2(1 + \varepsilon_1) = \rho_0$ represent the law of mass conservation for infinitesimally short thread elements at the two bar edges (length of thread element changing from ds_3 to ds_2 and density of thread material changing from ρ_3 to ρ_2 as bar moves

down through distance vdt within an infinitesimally short time dt; ρ_0 - initial density prior to impact; ε_1 - strain of both remaining upper horizontal thread segments, ε_3 - strain of horizontal thread segment under bar, ε_2 - strain along both intermediate thread segments sloping at angle φ). Two equations represent the law of momentum conservation under tension force T for infinitesimally short thread elements at the two bar edges, assuming that the friction force N and the pressure force P are related to each other in accordance with Coulomb's law of dry friction. The fifth equation represents Hooke's law. The problem is solved for unknown horizontal velocities $(dx/dt)_{1,2,3}$ and vertical velocities $(dy/dt)_{1,2,3}$ of thread particles, lengths of infinitesimal thread elements $ds_{2,3}$, strains $\varepsilon_{1,3}$, and forces $T_{2,3}$, P, $P_{x,y}$, $N_{x,y}$. This is done by reducing it to transcendatal equations of the general $F(v,\varphi) = 0$ form. As a special case is considered impact of a rough incident bar surface on a thread without slip under that surface. The results of a numerical analysis reveal that in the case of friction (coefficient $f > 0$) and an acute thread sloping angle ($0 < \varphi < \pi/2$) the strain ε_3 of the thread segment under the bar is larger than the strains of all its other segments. This strain decreases, while the strain ε_1 of both remaining upper horizontal thread segments increases as the thread sloping angle φ increases or when the friction coefficient f is increased. Figures 2; references 7.

Formation of Images of Spherical Objects in Acoustic Microscopy

927J0063A Moscow AKUSTICHESKIY ZHURNAL in Russian Vol 37 No 4, Jul-Aug 91 pp 702-708

[Article by P. V. Zinin and O. I. Lobkis, Institute of Physical Chemistry imeni N. N. Semenov, USSR Academy of Sciences]

UDC 534.26

[Abstract] Acoustic microscopy of spherical objects is considered, this method of microstructural examination having been so far applied to plane objects such as layers and interfaces only. An acoustic scanning reflection microscope is considered. Interaction of an acoustic wave emitted by a spherical focusing radiator-scanner (aperture angle 2α, radius of curvature f) and a spherical object (radius r) is analyzed, assuming that the radiator-scanner has a diameter much larger than the wavelength of emitted sound. The problem is defined in two Cartesian systems of coordinates: XYZ with origin O at the center of the radiator-scanner and X'Y'Z' with origin O' at the center of the object, axes OX',OY',OZ' being correspondingly parallel to axes OX,OY,OZ. Without loss of generality, the XOZ plane is shifted in the Y-direction till it coincides with the X'O'Z' plane so that both origins lie in that common plane and the distance between them is $(z_s^2 + r_s^2)^{1/2}$)(z_s along Z-axis, acoustic axis, and r_s along X'-axis). By virtue of the resulting axial symmetry (coaxial radiator-scanner and object configuration), coordinates z_s,r_s completely define the location of the object during a scan. The acoustic field potential at any point M in space near the focus of the radiator is equal to $v_0/2\pi$ times the surface integral of $(e^{ikp}/\rho)dS$ (v_0 - velocity of particle on radiator-scanner surface S, distance from point M to point N on radiator-scanner surface $\rho = R - r$, R - distance NO'from point N to center of object, r - distance MO' from point M to center of object, wave number $k = \omega/c$, ω - frequency of acoustic wave, c - speed of sound in immersion fluid. In a spherical system of coordinates r,θ,φ with origin O' at the center of the object, the spherical acoustic wave e^{ikp}/ρ is resolvable into a series $\Sigma_{n=0}^{\infty}\Sigma_{m=0}^{n}$ of spherical harmonics (products of spherical Hankel function of first kind $H_n(kR)$ by spherical Bessel function of first kind J_n (kr) by normalized associated Legendre polynomials P[dash over P]$_n^m(\cos\theta_R$P[dash over P]$_n^m(\cos\theta)\cos(m(\varphi_R - \varphi)$ by $2 - \delta_{0m}$, δ_{0m} - Kronecker delta). The performance of such an acoustic microscope using water as immersion fluid is evaluated on this basis, in the Fraunhofer diffraction approximation. The amplitude of the scanner output signal is calculated as a function of kz_s and of kr_s for two small solid spheres with ka = 0.1 (density 1 g/cm^3, speed of sound 1.57 km/s; density 1.2 g/cm^3, speed of sound 1.31 km/s), a perfectly rigid sphere with ka = 15, and two liquid spheres (density 0.93 g/cm^3, speed of sound 1.77 km/s) with ka = 14 and ka = 14.8 (resonance) respectively. Figures 5; references 10.

Propagation of Nonlinear Magnetoacoustic Waves Through Dissipative Electric Conductor Media With Drag

927J0063B Moscow AKUSTICHESKIY ZHURNAL in Russian Vol 37 No 4, Jul-Aug 91 pp 717-722

[Article by S. V. Korsunskiy, Institute of Hydromechanics, UkSSR Academy of Sciences]

UDC 533.951:532.546

[Abstract] Propagation of nonlinear magnetoacoustic waves through a compressible liquid electric conductor in a constant magnetic field and subject to a drag force dependent on the flow velocity is analyzed for the effect of dissipation in such a medium on evolution of perturbations and on formation of weak shock waves. The analysis is based on a system of MHD equations (G. Valenti; PHYSICS LETTERS Vol 134A No 7, 1989. S.V. Korsunskiy; AKUSTICHESKIY ZHURNAL Vol 36 No 1, 1990), equations describing one-dimensional propagation of such waves in a two-dimensional velocity field, in the adiabatic approximation. In the limiting case of $\sigma = \infty$ ($\nu_m = 0$) this system of equations is of the hyperbolic kind and can have solutions which describe propagating discontinuities. First is considered propagation of infinitesimally small MHD-field perturbations, a dispersion equation being obtained and solved for perturbations of the $e^{i(\omega t - kx)}$ form when $\eta,\nu_m << 1$ (η - dissipation factor, $\nu_m = 1/\mu\sigma$, μ - magnetic permeability, σ - electrical conductivity). Next is considered a strongly conducting liquid with a drag force linearly dependent

on the longitudinal velocity component in scalar terms. The evolution equation for this case, derived from that system of MHD equations by the Taniuti-Wei method (T. Taniuti and C.C. Wei; JOURNAL OF PHYSICS SOCIETY JAPAN, Vol 241, 1968) or by the Rudenko-Soluyan-Khokhlov multiscale method (O.V. Rudenko, S.I. Soluyan, and R.V. Khokhlov; AKUSTICHESKIY ZHURNAL Vol 20 No 3, 1974), is a Burgers perturbation equation which for the limiting case of $\eta = 0$ reduces to the classical Burgers equation and the Cauchy problem for which is solved here asymptotically for $\eta << 1$. The results indicate that in a magnetic field and in the presence of a drag force, dissipation losses will give rise to weak shock waves even when both kinematic viscosity and magnetic viscosity of the liquid are negligible. References 18.

Focusing Strong Acoustic Pulses

927J0063C Moscow AKUSTICHESKIY ZHURNAL in Russian Vol 37 No 4, Jul-Aug 91 pp 760-769

[Article by O. A. Sapozhnikov, Department of Physics, Moscow State University imeni M. V. Lomonosov]

UDC 634.222

[Abstract] Focusing of nonlinear acoustic pulse waves for applications such as an extracorporeal lithotrypter is analyzed by numerical simulation on the basis of appropriately approximated Khokhlov-Zabolotska equations, which describe focusing of strong sound pulses in a cylindrical system of coordinates. As a starting point is considered a linear acoustic pulse wave, a given focused pulse entering a given medium with a Gaussian radial amplitude distribution at the entrance and then propagating through it. A weak nonlinearity is then added and the focusing of such a pulse wave, assuming this wave to be a spherical one, is analyzed by subdividing the medium into two regions along the propagation path. In the initial region the wave remains nonlinear and is not diffracted. In the focal region the wave diffracted according to a linear law, this region extending sufficiently far for the wave degenerate into a linear one. A model of propagation of strong acoustic pulses with shock fronts is constructed on this basis which takes into account dependence of the pulse front velocity on the pulse front amplitude. In accordance with this model are calculated pulse profiles in the focal plane and pulse form transformations during propagation, a triangular pulse form having been selected because it represents the nonlinear asymptotic limit for the pulse form of any unipolar excitations. The author thanks O. V. Rudenko for discussion and M. M. Saratov for assistance in calculations. Figures 6; references 11.

Calculation of Acoustic Field in Nonuniform Waveguide by Method of Ray Acoustics

927J0063D Moscow AKUSTICHESKIY ZHURNAL in Russian Vol 37 No 4, Jul-Aug 91 pp 782-788

[Article by V. N. Fokin and M. S. Fokina, Institute of Applied Physics, USSR Academy of Sciences]

UDC 534.23.1

[Abstract] A fast and accurate algorithm for calculation of the acoustic field distribution in a nonuniform waveguide such as the ocean by the method of geometrical acoustics is proposed which involves two adjacent "basal" rays of the same class rather than a "basal" ray and a "target" ray so that tedious computation of the "target" trajectory has been eliminated. In the POLE program written for this algorithm the focusing factor $F = r.\cos\chi_1/|\delta r/\delta\chi_1|\sin\chi$ is used for calculation of the amplitude of an individual ray and the relation $\varphi = 2\pi dT + \pi(2k_s + k_c)/2 + \Sigma_{i=1}^{kb} A_{vi}$ is used for calculating its phase at the reception point (r - horizontal distance from source to reception point, χ_1 - angle of ray departure from source, χ - angle of ray incidence to reception point, f - frequency of emitted sound signal, T - travel time from source to reception point, k_b - number of reflections by waveguide bottom, k_s - number of reflections by waveguide surface, k_c - number of intersections with caustics, A_{vi} - phase of reflection coefficient at waveguide bottom. Both coherent and noncoherent fields at the reception point (x_r, z_r) are then calculated by adding in each case the contributions of all individual incoming rays, their characteristics at the reception point being obtained by linear interpolation according to the formula $X = [(z_1 - z_{i-1}/(X_i - X_{i-1}]^{-1}] (z_r - z_i)$ (z - depth of reception point). The program was used for evaluating the dependence of three principal characteristics of a "basal" ray (length of ray arc R, sine of incidence angle at reception point $S = \sin\chi$, and travel time T) on the depth of the reception point at some horizontal distance r (60 km) from the source. The results of test calculations are compared with results obtained using two conventional programs involving a "basal" ray and a "target" ray (RAY program, A. V. Bagin, "Mozaika" 1973-74; DELTA, A. L. Piskarev, 1988-89). As a specific example for numerical analysis is considered an oceanic waveguide with an acoustically soft free surface and an uneven liquid bottom, a 240 Hz sound source being located 284 m deep below the surface. The authors thank I. A. Shershevskiy, N. A. Zavolskiy, and A. G. Sazontov for supplying data on RAY and DELTA programs, also for facilitating calculations based on the parabolic equation. Figures 6; references 7.

Phase Conjugation of Sound Beams During Four-Wave Interaction in Liquid With Gas Bubbles

927J0063E Moscow AKUSTICHESKIY ZHURNAL in Russian, Vol 37 No 4, Jul-Aug 91 pp 815-817

[Article by N. P. Andreyeva, K. Karshiyev, and L. M. Sabirov, Department of Physics, Samarkand State University imeni A. Navoi]

UDC 534.222

[Abstract] Phase conjugation of sound beams by four-wave interaction in a liquid with gas bubbles was studied in an experiment with an electrolytic bubble generator

and two piezoceramic 3 MHz sound radiators in a water tank, both radiators being immersed in water outside the bubble column. One radiator was located in the upper part of the tank and emitted a horizontal beam of pump waves. The other radiator was located in the lower part of the tank and emitted a beam of signal waves in pulses of 100 μs duration at a repetition rate of 160 Hz, the beam sloping upward at an angle ensuring intersection of the two beams entirely within the vertically rising bubble column. The signal radiator was also used as transducer for measuring the amplitude of scattered sound so that, owing to the time shift between emission of a signal wave and reception of scattered sound, it was possible to also measure the amplitude of the sound component returning with reversed wavefront. For the purpose of determining the dependence of the reflection coefficient on the bubble concentration, the latter was varied by varying the electrolyzer voltage over the 5-50 V and the amplitude of the scattered signal had to be averaged because of unavoidable instability of the bubble column. An about 2 percent scattering of the pump wave was recorded in absence of a signal wave. No scattering of the signal wave was recorded in absence of bubbles. Maximum scattering was recorded at voltages of 30-50 V and the reflection coefficient remained constant at R = 0.3 over this entire range, probably because of bubble concentration saturation. Figures 3; references 3.

Collision-Radiative Generation of Sound in Methyl Alcohol Vapor

927J0078A Moscow PISMA V ZHURNAL EKSPERIMENTALNOY IN TEORETICHESKOY FIZIKI in Russian Vol 54 No 4, 25 Aug 91 pp 216-219

[Article by A. Ye. Bakarev, F. Kh. Gelmukhanov, and A. M. Sinyukov, Institute of Automation and Electrometry, Siberian Department, USSR Academy of Sciences, Novosibirsk]

[Abstract] Sound in a gaseous medium was, for the first time ever, generated by means of light-induced drift and light-induced thermal flux in an experiment with CH_3OH vapor. This phenomenon is now explained theoretically on the basis of resonant interaction of light with a binary gaseous mixture, one component of the mixture absorbing the light and the other component acting as buffer only. Acoustic vibrations in such a medium are described by the wave equation for an excess pressure δp to the total pressure of the mixture, disregarding weak light-induced diffusion effects. On the basis of this equation is estimated the ratio $\delta p_{lid}/\delta p_{tot} \approx (\nu/\nu_{crit})^2$ (p_{lid} - pressure due to light-induced drift, p_{tot} - total pressure, ν - frequency of light-intensity modulation, ν_{crit} - "critical" frequency), the "critical" frequency depending on the gas temperature T, the mass of each component $m_{a,b}$, the light absorption length l_0, and the de-excitation frequency ν_d. The theory indicates that collision-radiative generation of sound can also take place in a one-component gaseous medium. The experiment was performed with a CO_2-laser tunable over an about 300 MHz wide frequency range by means of a diffraction grating at an about 1 W power level, and with an optoacoustic resonance cell. A barrier inside the cell split it into two parallel channels forming a U, for passage of the "forward" laser beam and the "reverse" laser beam. In the lateral wall along the "forward" laser beam was seated an MKE-3 microphone. Both channels were closed on each end by a KBr window. The laser was operating at the 9P16-line wavelength, closest to the $R(0,0;11)^{CO} \rightarrow (0,0;10)^0$ transition in a CH_3OH molecule. Its radiation was amplitude-modulated by means of an ML-7 electrooptic modulator. After a Ge plate behind the modulator split the laser beam into "forward" one and the "reverse" one, a set of mirrors returned the "reverse" beam into its channel so that both beams had equal diameters. The cell was filled with pure CH_3OH vapor and, for comparison, with CH_3OH + Xe or H_2 mixture in a 1:1 ratio. The cell was excited to its 18 kHz resonance frequency, assuming this to be its Helmholtz frequency. In order to detect the much weaker sound generated by the collision-radiative mechanism, it was necessary to suppress the sound generated by the optoacoustic mechanism. This was achieved by having the two laser beams propagate in opposite directions and by properly balancing their intensity so that only the collision-radiative sound signal would be amplified. This could not be achieved at other frequencies, 18 kHz thus definitely being the Helmholtz frequency. Sound was also generated in this cell with only one laser beam, for recording the contour of the δp_d absorption line of CH_3OH vapor and with two opposing laser beams for recording the spectrum of the δp_{lib} line. Figures 3; references 12.

High-T_c Superconductor Phase in $Fe_{1-x}S$ System

927J0078B Moscow PISMA V ZHURNAL EKSPERIMENTALNOY I TEORETICHESKOY FIZIKI in Russian Vol 54 No 4, 25 Aug 91 pp 224-227

[Article by G. A. Petrakovskiy, G. V. Loseva, N. I. Kiselev, S. G. Ovchinnikov, N. B. Ivanova, and V. K. Chernov, Institute of Physics, Siberian Department, USSR Academy of Sciences, Krasnoyarsk]

[Abstract] An experimental study of intermediate phases in the $Fe_{1-x}S$ sulfide system ($0.07 < x \leq 0.125$) was made concerning the temperature dependence of their electrical resistivity and magnetic susceptibility over the 4.2-300 K range. Polycrystalline specimens of x = 0.074, 0.083, 0.091, 0.111, and 0.125 phases were produced from pure Fe and S in quartz flasks under vacuum. X-ray analysis at 300 K revealed a monoclinic Fe_7S_8 structure, i.e., NiAs(4c) superstructure of the x = 0.125 phase, close to Fe_8S_9 structure (5C superstructure) of the x = 0.111 phase, similar and close to NiAs(1c) structures of x = 0.091 and x = 0.083 phases. X-ray and differential thermal analyses revealed a close to FeS structure (2C superstructure) of the x = 0.074 phase at 300 K. The results of electrical resistivity measurements indicate a semiconductor-like behavior of both x = 0.125 and x = 0.111 phases, the electrical resistivity of the x = 0.125 phase peaking to a maximum within 100-110 K and that

of the x = 0.111 phase decreasing monotonically as the temperature rises but at a faster rate as the temperature rises above 110 K. The results of magnetic susceptibility measurements (X' - real part of complex initial susceptibility) indicate that the three x = 0.125, x = 0.111, and x = 0.091 phases become more paramagnetic as the temperature falls from 300 K to 128 K and then, owing to a diamagnetic effect, become less paramagnetic as the temperature falls further below 128 K. This diamagnetic effect is strongest in the x = 0.125 phase and weakest in the x = 0.091 phase. The two x = 0.083 and x = 0.074 phases are weakly paramagnetic throughout the entire temperature range, their X' being smaller than 0.01 and remaining constant. It is noteworthy that the 128 K temperature at which diamagnetism begins, and at which superconducting transition thus begins to occur, is higher than the temperature at which the electrical resistivity begins to decrease. Partial diamagnetism especially in the x = 0.125 phase is also indicated by a change in the shape of the hysteresis loop as the temperature passes through that T_c = 128 K point. The authors thank A. V. Baranov for performing the X-ray structural analysis, also A. D. Balayev and M. M. Karpenko for measuring the hysteresis loops. Figures 3; references 9.

Wave Phenomena in Drawn Strip

927J0084B Kiev PRIKLADNAYA MEKHANIKA in Russian Vol 27 No 9, Sep 91 pp 114-119

[Article by V. P. Boldin, M. V. Trubin, Gorkiy Department of the Mechanical Engineering Institute at the USSR Academy of Sciences]

UDC 534.1

[Abstract] The dynamic behavior of two-dimensional elastic systems with a moving load and constraints and the manifestations of wave phenomena in such systems, particularly the multiple repetition of wave phenomena which under certain conditions may accumulate and lead to a qualitative change in dynamic behavior, i.e., instability and pulsed vibrations, are considered. Using a strip simulated by the lateral vibration equation of a rectangular membrane with distributed losses with two absolutely rigid constraints moving along it, the manifestations of a number of wave phenomena are analyzed and for the first time, the possibility of the vibration energy amplification of damping is demonstrated. Formulas are derived for the resonance frequency and tractive resistance as a function of the strip velocity. The results indicate that the phenomena occurring in the strip can be explained most naturally by wave concepts. The aberration, resonance frequency shift, energy enhancement, and the constraints' tractive resistance are attributed to the Doppler effect. The resulting expressions may be used for finding optimal operating conditions of rotary presses and conveyor belt transport mechanisms and other devices. Figures 2; references 11.

Shock Wave Parameters of Explosively Expanding Boiling Liquid

927J0085A Moscow FIZIKA GORENIYA I VZRYVA in Russian Vol 27 No 4, Jul-Aug 91 pp 51-57

[Article by S. P. Medvedev, A. N. Polenov, B. Ye. Gelfand, Moscow]

UDC 534.222.2+532.542.2

[Abstract] Interest in studying the parameters of shock waves (UV) forming in the environment of a superheated liquid when its volume suddenly begins to expand is attributed to the need to simulate an emergency situation with a coolant leakage where intensive evaporation commences after the system becomes depressurized. The parameters of planar shock waves forming during the expansion of a superheated liquid are investigated in a shock tube with a heated high-pressure chamber. The process of liquid component vaporization makes the principal contribution to the shock wave compression phase momentum during the expansion of the stratified liquid-saturated vapor system. The shock wave amplitude is determined by the pressure ratio of the expanding liquid volume and the ambient space and almost does not depend on the liquid properties. The shock wave pulse duration is proportionate to the mass of the liquid. The design of the experimental unit is described. A procedure for calculating the shock wave intensity is proposed; analytical results obtained by this procedure are consistent with experimental data. Figures 5; tables 1; references 8: 7 Russian, 1 Western.

Decomposition Characteristics of Compressed PETN Charges Under Dynamic Starting Pulses

927J0085B Moscow FIZIKA GORENIYA I VZRYVA in Russian Vol 27 No 4, Jul-Aug 91 pp 65-72

[Article by G. S. Andreyev, A. Ye. Novitskiy, V. S. Solovyev, Moscow]

UDC 534.222.2

[Abstract] The quasithin explosion (VV) layer (KTS) method is used to investigate the decomposition characteristics of pentaerythrityl tetranitrate (TEN), both pure and phlegmatized, under the effect of dynamic starting pulses (NI) with step and multistep leading edges. The starting pulse is understood as the pressure variation law on the pressure application plane. An analysis shows that in charges with initial porosity, the behavior of the combustion surface and, consequently, the decomposition rate are affected not only by the concentration of igniting hot spots and their distribution in space and the rate of layer-by-layer combustion but also by the rate of "filtering", i.e., the combustion product propagation in the shock-compressed explosive. These data are useful for expanding model concepts and describing the localized decomposition of porous explosives by shock waves. It is speculated that the decomposition rate of an

elementary cell of the reacting mixture formed from a structurally inhomogeneous explosive in a general case is determined not only by the instantaneous value of pressure and the rate of its change but also the energy source responsible for the change in pressure, i.e., external or internal, in relation to the elementary cell itself. Figures 4; references 15.

Effect of Charge Strength on Ignition Parameters of Solids Under Shock

927J0085C Moscow FIZIKA GORENIYA I VZRYVA in Russian Vol 27 No 4, Jul-Aug 91 pp 99-104

[Article by M. V. Lisanov, A. V. Dubovik, Moscow]

UDC 531.663

[Abstract] Methods of estimating the sensitivity of solid explosives to mechanical action by the critical stress criteria and a set of standard methods based on determining the explsotion frequency or probability are discussed and an attempt is made to determine the factors affecting the measurement accuracy of explosive sensitivity indices and thus explain why data obtained by various researchers are inconsistent. To this end, a model of thermoplastic failure and ignition of a thin layer of viscoplastic material by a low-speed shock is used to compute numerically the initiation parameters and explosion probability rate curves as a function of the charge dimensions and shock energy. It is assumed that the explosive layer compression is uniaxial and axisymmetric; the melting point depends linearly on pressure and is on the boundary of mechanical heating of the explosive material; the charge failure time is shorter than the sound wave travel time through the impact testing machine system; and the maximum heating is localized in the shear plane near the contact boundary of the charge and the striker. The charge strength is assumed to be normally distributed. The possibility of lowering the critical explosion ignition pressure by adding a fluid low-strength phlegmatizing component to the explosive is demonstrated. Figures 2; references 9.

Shock Compaction of Diamond Powder

927J0085D Moscow FIZIKA GORENIYA I VZRYVA in Russian Vol 27 No 4, Jul-Aug 91 pp 139

[Article by S. S. Batsanov, V. A. Vazyulin, L. I. Kopaneva, I. P. Maksimov, V. A. Morozov, S. L. Fomin, A. S. Shmakov, Mendeleyevo]

UDC 534.411

[Abstract] The use of the method of dynamic-static compression for explosion shock compaction of diamond powder is described. The detonation rate in a cylindrical experimental unit reaches 7.6 km/s; electric contact pickups are used to evaluate the dynamic pressure and to measure the shock wave velocity. The mean measurement interval, i.e., the time between the closing of the pickup circuit, is 0.75 μs +/- 6 percent which corresponds to a shock wave velocity of 8 km/s. A 15 kbar static pressure is applied during the dynamic pressure release phase for one hour. As a result, a solid tablet with a 3.32 g/cm^3 density and a Vickers hardness number of 5,000 is produced. An X-ray picture demonstrates that the characteristics of the resulting item are almost identical to those of the original powder except for a certain line constriction. References 2.

Metal-to-Insulator Transition in Amorphous GaSb

927J0067D Moscow ZHURNAL EKSPERIMENTALNOY I TEORETICHESKOY FIZIKI in Russian Vol 100 No 8, Aug 91 pp 707-724

[Article by S. V. Demishev, Yu. N. Kosichkin, D. G. Lunts, A. G. Lyapin, N. Ye. Sluchanko, and M. S. Sharambelyan, Institute of General Physics and Institute of High-Pressure Physics imeni L. F. Vereshchagin, USSR Academy of Sciences]

[Abstract] An experimental study of amorphous a-GaSb production by quenching crystalline c-GaSb under high pressure was made, for the purpose of examining the process conditions (pressure p_s, temperature T_s, quenching rate dT/dt, post-quenching pressure reduction rate dp/dt) necessary for amorphization of this semiconductor compound and determining its properties in the superconducting state. Specimens for this study were prepared by a combination high-pressure and high-temperature treatment compatible with the p-T phase diagram. Intrinsic GaSb single crystals cut into disks not more than 1.5 mm thick and about 2.5 mm in diameter were placed in a high-pressure high-temperature chamber of the "Toroid" for 30-60 s long period and then quenched to room temperature under constant pressure. The pressure was then slowly, over an about 600 s long period, lowered to atmospheric level. Contamination of the chemically aggressive GaSb melt was effectively prevented by having the single crystal placed in an insulating container made of NaCl. Structural examination was done by recording X-ray debyegrams and processing them in a specially designed microdensitometer. Galvanomagnetic measurements covering the 1.8-630 K temperature range in a magnetic field of up to 150 kOe intensity were made by the standard method using a Bitter magnet. The data on the structural characteristics indicates that most critical requirement for amorphization of GaSb is that the pressure p_s be above the approximately 60 kbar pressure corresponding to transition from GaSb-I phase with a diamond crystal lattice to GaSb-II phase with a β-Sn crystal lattice, amorphization being altogether impossible under pressure below that transition pressure. Under pressures above 70 kbar, moreover, large disordering of the structure occurs at treatment temperatures from 400°C to 1400°C. Variation of the quenching rate from 1 K/s to 1000 K/s does not significantly influence the structure and the physical properties. It was not technically possible to vary the rate of post-quenching pressure reduction dp/dt over a sufficiently wide range and, therefore, it was set at approximately 1 kbar/s. Considering the essential role of the composition of the $(a\text{-}GaSb)_{1-X}(c\text{-}GaSb)_X$ system characterized by the parameter X in the interpretation of the findings, this parameter was calculated on the basis of X-ray scattering data in accordance with the principle of scattering intensity conservation. An analysis of the results reveals that while the structural characteristics of a-GaSb are determined by a treatment process pressure p_s as the principal factor, its electrophysical properties are almost fully determined by the treatment process temperature T_s. The electrical resistivity ρ and its temperature dependence are found to become very different after the treatment process temperature T_s has been changed from above 800°C to below 800°C, switching from a metal-like behavior after treatment at $T_s > 800$°C to an insulator-like behavior after treatment at $T_s < 800$°C. On the dielectric side of the transition, the temperature dependence of the electrical resistivity ρ(T) follows the activation law in the $T > 100$ K range and Mott's law in the $T \leq 20$ K range. Evidently, however, this metal-to-insulator transition cannot be explained by change in the composition alone and the behavior on the metallic side of the transition also needs to be considered. On this side, after treatment at $T_s > 800$°C, the data reveal that the metal-like behavior characterized by weakly temperature-dependent electrical resistivity ρ down to about 10 K is followed by transition to a superconducting state which begins at about 7 K and ends with zero electrical resistivity at about 1.8 K (residual 0.0001ρ). The magnetoresistivity and the magnetic susceptibility after treatment at $T_s = 1000$°C were measured in a magnetic field of up to 150 kOe intensity at temperatures covering the 7-1.8 K range, for an evaluation of their field and temperature dependence. The current dependence of the electrical resistivity ρ(i) within this temperature range was determined from the current-voltage characteristics measured with a constant direct current ranging from $i < 0.1$ mA to $i > 0.10$ A. The results of all these measurements indicate that a-GaSb becomes a type-2 superconductor. For the purpose of evaluating and separating Joule-effect heating, the current-voltage characteristics were also measured with current pulses, their amplitude varied from about 0.01 A up to 10 A and their duration selected so as to ensure that the temperature rise ΔT (proportional to i^2R) be two orders of magnitude smaller than with constant current. A comparison of the ρ(i) curves indicates that at 2.5 K temperature Joule-effect heating begins when the current exceeds 0.1 A. The corresponding sharp rise of electrical resistivity may, however, be caused not only by heating but also by the current mechanism of superconductivity annihilation. The authors thank A. A. Abrikosov for discussing several aspects of this study, also S. V. Popova and V. V. Brazhin for support and assistance in preparation of the a-GaSb specimens. Figures 9; references 25.

Excitons in Incompressible Fluid: Giant Polaron Effect

927J0069B Moscow PISMA V ZHURNAL EKSPERIMENTALNOY I TEORETICHESKOY FIZIKI in Russian Vol54 No 3, 10 Aug 91 pp 160-165

[Article by V. M. Apalkov and E. I. Rashba, Institute of Theoretical Physics imeni L. D. Landau, USSR Academy of Sciences, Moscow]

[Abstract] In connection with optical spectroscopy of an incompressible two-dimensional fluid and the attendant fractional quantum Hall effect, it is demonstrated theoretically that phonons or magnetotrons of such a fluid

produce a strong and very specific polaron effect: giant renormalization of the exciton dispersion law when there is a momentum $k > 0$ (no shift of energy level when $k = 0$ in the symmetric electron-hole interaction model). The proof is based on conclusions drawn from an analysis of the electron-hole interaction Hamiltonian, which includes Fermi electron and hole annihilation operators in the Landau gauge with interaction potentials $V_{eh} = -V_{ee} = -V_{hh}$ in the symmetric model. Accordingly, to each state of the electron-hole state there corresponds one with an additional electron-hole pair in the form of an exciton. Excitons interact with phonons when there is a momentum $k > 0$, the strength of this interaction being proportional to that momentum. Calculations are shown for a system of five electrons + one hole in a spherical configuration ($k = L/R$, L - angular momentum, R - radius of sphere, $R^2 = 2S$, S - Haldene's parameter). They indicate a giant suppression of exciton dispersion $\varepsilon^*(k)$ in the presence of an incompressible two-dimensional fluid when $k < 1$, the optical spectrum in the quantum limit being trivial and coinciding with the spectrum of a free exciton. When the momentum is very small, $k \approx 1$, then local modes analogous to two-dimensional and three-dimensional polarons then appear in the vicinity of an exciton so that the latter loses its distinctiveness. When the latent symmetry has been broken by slanting the quantum well so that the maximum hole concentration is approximately equal to the maximum electron concentration, then the polaron effect manifests itself already in absence of a momentum ($k = 0$). In the presence of a very small momentum $k << 1$ in this case, the shielding of a hole weakens and states near the bottom of the energy spectrum assume the dominant role so that the optical spectrum becomes nontrivial and dependent on the occupation factor $\nu < 1$. Figures 2; references 21.

Magnetization of Frustrated Two-Dimensional Heisenberg Antiferromagnetic Material: Analogy to Fractional Quantum Hall Effect

927J0070B Moscow PISMA V ZHURNAL EKSPERIMENTALNOY I TEORETICHESKOY FIZIKI in Russian Vol 54 No 2, 25 Jul 91 pp 94-96

[Article by Yu. Ye. Lozovik and O. I. Notych, Institute of Spectroscopy, USSR Academy of Sciences, Troitsk (Moscow Oblast)]

[Abstract] A frustrated two-dimensional Heisenberg antiferromagnetic material with ½ spin is considered at zero temperature in an external magnetic field sufficiently strong for aligning most or all spins with it. The magnetization of such an antiferromagnetic material was calculated for a 4x4 square two-dimensional lattice with periodic boundary conditions, with the spin-spin and spin-field interaction Hamiltonian exactly diagonalized and with frustration introduced by including interaction of next behind the nearest spins. The frustration factor $r = J_1/(J_0 + J_1)$ (J_0 - exchange interaction of nearest neighboring spins, J_1 - exchange interaction of next behind nearest spins) was varied over the $0 \leq r \leq 1$ range, a long-range Neel order existing when $r = 0$ and the lattice being divisible into two noninteracting sublattices with a long-range order in each when $r = 1$. A phase transition occurs when $r \approx 0.35$ and the frustration is maximum. The field dependence of magnetization in the two most characteristic cases of $r = 0$ and $r = 0.35$ is described by a ladder curve, each step corresponding to a reversal of one spin and thus an increase of magnetization by unity. These steps are uniform when $r = 0$, while some increase and some decrease when $r = 0.35$ but they become smoother as the lattice dimensions are increased so that for large lattice there appear plateaus along the ladder. They appear where magnetization M is equal to M_{max}, M_{max}, and $3M_{max}$. Their lengths depend on r and the maximum length corresponds to maximum frustration. All this indicates that some states with specific magnitudes of magnetization are more stable than others and that the system will remain in those stable states at a sufficiently high intensity of the magnetizing field. This phenomenon is analogous to incompressibility of fractional quantum Hall effect states with rational values of ν. The authors thank A. B. Kashuba for helpful discussions and A. S. Semenov for assistance. Figures 1; references 6.

Superconductors With Quasi-Localized Bismuthate-$A^{IV}B^{VI}$:Me^{IIIb} (Metal-Doped Semiconductor) Pairs

927J0072A Leningrad FIZIKA TVERDOGO TELA in Russian Vol 33 No 2, Feb 91 pp 350-357

[Article by M. V. Krasinkova and B. Ya. Moyzhes, Institute of Engineering Physics imeni A. F. Ioffe, USSR Academy of Sciences, Leningrad]

UDC 537.312.62

[Abstract] Superconductivity of materials consisting of quasi-localized bismuthate and $A^{IV}B^{VI}$:Me^{IIIb} metal-doped semiconductor pairs is analyzed theoretically, among the pure $A^{IV}B^{VI}$ compounds superconductivity being exhibited only by nonstoichiometric $Sn_{1-d}Te$ (T_c about 0.2 K) and nonstoichiometric $Ge_{1-d}Te$ with a hole concentration $p \infty 10^{21}$ cm^{-3} (T_c about 0.4) K but not by PbTe, PbSe, and PbS unless doped with a metal of the IIIb group. Among the bismuthates, superconductivity is known to be exhibited only by two compounds with a high Bi content, namely $BaPb_{1-x}Bi_xO_3$ ($T_c \infty 12$ K when $x \infty 0.25$) and $Ba_{1-x}K_xBiO_3$ ($T_c \infty 30$ K when $x = 0.4$), while the respective constituent compounds $BaPbO_3$ (metal-like behavior) and $BaBiO_3$ (insulator-like behavior) do not exhibit superconductivity at all. Following a description of $BaPbO_3$, $BaBiO_3$, and $A^{IV}B^{VI}$:Me^{IIIb} (Me = In,Tl) semiconductors in terms of energy bands theory and lattice structure, the parameters on which the critical superconducting transition temperature for these bismuthate-$A^{IV}B^{VI}$:Me^{IIIb} materials depends on, and are evaluated on the basis of, the BCS theory and on the premise that superconductivity is attributable to Bloch electron subsystem. The energy gap

in the spectrum of impurity states in those semiconductors and localization of carriers in the bismuthates are evaluated accordingly, with reference to available data and considering the existence of ready diamagnetic pairs as well as Cooper pairs available to participate in the superconducting. It is found that two-electron quasi-localized states forming during disproportionation of s^1 ions according to the $2s^1 \rightarrow s^0 + s^2$ scheme can stimulate superconduction, as they do in cuprates. Transition of these bismuthates and the $A^{IV}B^{VI}$:Me^{IIIb} semiconductors into the superconducting state evidently requires that the Fermi level be located within the band of two-electron states and thus requires approximately equal concentrations of s^0 and s^2 ions. Figures 3; references 22.

Randomization of Motion of Relativistic Electrons Along Axis of Single Crystal

927J0073B Leningrad ZHURNAL TEKHNICHESKOY FIZIKI in Russian Vol 61 No 5, May 91 pp 65-71

[Article by B. R. Meshcherov and V. I. Tumanov]

[Abstract] The nuclear reaction attending short-range collisions during passage of relativistic electrons with energy above the potential barrier through a silicon crystal along one of its principal axes was studied in an experiment involving measurement of the reaction yield, within the range of intense mixing of above-barrier and below-barrier fractions when electrons of the latter fraction have enough time to move through the mean path from one reversal point to another. An electron formed by the "Fakel (Torch)" pulsed linear high-current electron accelerator (Institute of Atomic Energy) was passed through a 50 m long electric conductor with turned-off magnetic optics and then through a collimator with a 20 mm in diameter aperture before it entered the target crystal. The target was a planar perfect Si:B (substitutional impurity) single crystal 64 mm in diameter with both front and back faces perpendicular to its [100] axis (within 0.5°), the impurity being necessary for anodic oxidation but its atomic concentration of about $2x10^{16}$ cm^{-3} being sufficiently small not to influence the dynamics of electron beam passage. The central part of the crystal was etched down into an about 50 μm thick and 56 mm in diameter web facing the collimator. The crystal was mounted on a goniometer with two degrees of freedom controlling the crystal orientation of the crystal relative to the incident electron beam. A rotatable triangular prismatic magnet behind the crystal on the common axis deflected the electron beam leaving the crystal into an absorber, while transmitting γ-quanta produced in the crystal and sending them through another collimator (with protective wall) to a detector. Hard radiation produced in the crystal was collimated within an angle equal to the reciprocal of the Lorentz factor. Electron bombardment of silicon produces only two long-lived β-active isotopes ^{24}Na and ^{28}Mg. The cross-sections for their production by $E \approx 47$ MeV electrons were found to be about $1x10^{-31}$ cm^2 and about $8x10^{-31}$ cm^2 respectively. The crystal was, after bombardment, sliced by successive formation of a thin homogeneous anodic oxide layer of given thickness on the surface and its subsequent removal by etching with hydrofluoric acid. Examination of the slices revealed three factors influencing the experiment and requiring corrective measures. Nonuniform thermal expansion of the crystal heated by the electron beam and resulting radial stresses can, at sufficiently high current levels, bend the crystal. This was avoided by coating the back face with soot and thus improving extraction of the heat through the back face, also by bombarding the crystal at a mean current level (13 μA) lower than the critical (16 μA). Escape of the highly mobile Na and Mg ions from the crystal during anodic oxidation, namely their migration into the electrolyte (800 ml H_2O + 200 ml glycerin + 12 g oxalic acid + 5 g H_eBO_3 + 0.5 g NH_4F), was accounted for in the selection of the process parameters: bombardment time about 7 h, thickness of silicon slice for each activity measurement about 0.17 μm, measuring time 3000 s. Radiative defects produced in the crystal during bombardment with an about 10^{18} cm^{-2} density were completely removed, along with the soot coating, by heat treatment at about 600°C for about 20 min without any noticeable diffusion taking place. Measurements of the two activities in the crystal were made with the crystal [100] axis first collinear with the incident electron beam and then at an approximately 1.5° angle to it. The data reveal a strong dependence of both activities and a weak dependence of their ratio on the penetration depth of relativistic electrons. The readings differ by almost an order of magnitude from the results of calculations based on the assumption of distinct states of electrons, which indicates an intense mixing of charged particles in the space of "transverse" energy and momentum levels as a result of strongly perturbing vibration of atom shells. This, in turn, indicates a highly randomized motion of charged particles in the crystal. The authors thank V. A. Bazilev for interest, V. V. Goloviznin for helpful discussions, S. P. Miroshinkova for consultations on planar chemical etching of silicon, and D. M. Levin for assistance in ellipsometry of slices. Figures 6; references 17.

Quantum Hall Effect on Holes in Ge-$Ge_{1-x}Si_x$ Strained Superlattices

927J0076C Moscow PISMA V ZHURNAL EKSPERIMENTALNOY I TEORETICHESKOY FIZIKI in Russian Vol 54 No 6, Sep 91 pp 351-353

[Article by O. A. Kuznetsov, L. K. Orlov, R. A. Rubtsova, A. L. Chernov, Yu. G. Arapov, N. A. Gorodilov, G. L. Shtrapenin, Applied Physics Institute at the USSR Academy of Sciences, Nizhniy Novgorod, Scientific Research Institute of Engineering Physics at the Nizhniy Novgorod University, and Metal Physics Institute at the USSR Academy of Sciences, Sverdlovsk]

[Abstract] The results of measurements of a new and unique physical phenomenon—the quantum Hall effect—on holes in a strained multilayered Ge-$Ge_{1-x}Si_x$

heterostructure, i.e., selectively doped superlattices (SR) obtained by the hybrid method, taken by various authors are summarized. Both Hall and magnetic transport measurements are described. The plateaus and oscillations on curves of the dependence of resistance in various planes on the magnetic field is attributed to the hole gas quantization in the superlattice's Ge layers. The review draws the conclusion that heterosystems on the basis of Ge-$Ge_{1-x}Si_x$, including superlattices, are a promising tool for investigating physical processes in two-dimensional systems and that examinations of the quantum Hall effect makes it possible to obtain valuable data on the characteristics of samples with a 2*D* free charge carrier gas. The authors are grateful to Ye. A. Uskova and Ye. V. Kirillova for making junctions and structures, B. A. Aronzon and O. A. Mironov for helpful cooperation, Yu. N. Drozdov for helping with X-ray diffraction analyses of the structures, and I. M. Tsidilkovskiy and V. A. Volkov for their help and for discussing the findings. Figures 1; references 5: 3 Russian, 2 Western.

Color Center Accumulation in CsBr Under Electron Irradiation and Recombination Thermostimulated Exoelectron Emission

927J0082B Kiev UKRAINSKIY FIZICHESKIY ZHURNAL in Russian Vol 36 No 11, Nov 91 pp 1737-1743

[Article by P. V. Galiy, V. P. Savchin, Lvov University imeni Ivan Franko]

UDC 539.21.539.12.04+537.532.2

[Abstract] Radiation-induced defects (RD) developing in alkali halide crystals (ShchGK) at various energy levels are discussed and the accumulation and annealing patterns of *F*- and *M*-color centers in nominally pure and doped alkali halide CsBr, CsBr-Cd crystals at high electron irradiation densities and doses when the concentration of the resulting color centers (TsO) is comparable to, or exceeds, that of the Cd^{2+} activator are investigated. Color centers developing under irradiation by electrons at $E = 10$ kEv in a pulse mode at 295K with $\tau = 20$ μs and $f = 50$ Hz are studied by the absorption spectrophotometry methods and the accumulation kinetics of electron *F*- and *M*-color centers and the kinetics of thermally stimulated exoelectron emission in a 295-600K range after various electron irradiation doses are studied. Optical transmittance is the main parameter studied by absorption spectrophotometry in the 400-1,000 nm band. The electron *F*-center concentration and the mean energy needed to create one such center are calculated within an absorbed radiation dose range of (7.7-36.6) x 10^6 gR/s and an electron irradiation dose range of (0.46-69.34) x 10^6 gR. A correlation of thermal annealing of color centers and peaks of thermally stimulated recombination exoelectron emission is established. Figures 3; tables 1; references 15: 13 Russian, 2 Western.

Spin Relaxation in Liquid Helium

927J0056A Moscow ZHURNAL EKSPERIMENTALNOY I TEORETICHESKOY FIZIKI in Russian Vol 100 No 1(7), Jul 91 pp 189-196

[Article by I. S. Solodovnikov, Institute of Problems in Physics imeni P. L. Kapitsa, USSR Academy of Sciences]

[Abstract] An experimental study of nuclear spin-lattice relaxation in liquid helium was made involving measurement of the relaxation time at temperatures covering the 0.04-0.7 K range with various amounts of ^{3}He in the cell. The cooling duct of the cell was screwed on to the copper lid of a refrigerator for ^{3}He + 0.015 percent ^{4}He solution, the liquid ^{3}He being cooled by means of a copper needle coated with In-Pb alloy and a sintered Cu powder with a surface area sufficiently large (0.14 m^2) for adsorption of ^{4}He. The total cell volume was 0.37 cm^3, the volume of the gauge region for measurements being 0.12 cm^3 large and bounded by a 1.4 cm^2 large surface area (area of cell "ceiling" 0.45 cm^2). Measurements were made with the cell charged to k = 1 (full), 0.75, and 0.50 capacity referring to volume of concentrated gas and magnetic moment of the liquid. The latter was measured with a high-frequency SQUID, nuclear-paramagnetic resonance being indicated by change of the longitudinal magnetization of the liquid upon adiabatic fast resonance line crossover as an alternating magnetic field with a 4 mOe amplitude was applied for about 40 s while its frequency was being swept at a rate of 25 Hz/s. Most measurements were made with the resonance frequency f = 37 kHz H_0 = 11.4 Oe. Some measurements were made with the resonance frequency f = 18 kHz and, at temperature near or equal to 0.70 K, with the resonance frequency lowered farther down to 2.5 kHz. The relaxation time was found not to depend on the frequency. It was determined on the basis of two successive crossovers with attendant magnetization reversal. In this way were determined the relaxation of the deviation of the magnetic moment from its equilibrium magnitude and the relaxation time. The subsequently evaluated temperature and fill factor dependence of the relaxation time τ(T,k) revealed that at temperatures below 0.17 K the longitudinal magnetization relaxed fastest in a half-full cell (k = 0.50), somewhat slower in a full cell (k = 1), and much slower when k = 0.75; at these temperatures the density of ^{3}He vapor above the liquid was negligible and the ceiling of the cell did not contribute to magnetization relaxation at its walls when k < 1. At temperatures above 0.30 K, the relaxation time increased monotonically with k, the density of saturated ^{3}He vapor being high and excess magnetization of the liquid being transferred by diffusion of vapor atoms to the ceiling of the cell. The relaxation time peaked to a maximum length within the 0.17-0.30 K range, the amount of additional magnetization transfer time being determined by the number of vapor atoms striking the surface of the liquid. Theoretical calculations based on diffusion theory have yielded a temperature dependence of the relaxation time along curves for k = 1, 0.75, 0.50 which fit the experimental points. The author thanks N. V. Zavaritskiy for interest and very stimulating discussions, and A. A. Yurgens for assistance. Figures 5; references 20.

Collective Excitation in Superfluid ^{3}He Planar 2*D* Phase

927J0064D Moscow ZHURNAL EKSPERIMENTALNOY I TEORETICHESKOY FIZIKI in Russian Vol 100 No 3(9), Sep 91 pp 849-854

[Article by P. N. Brusov, M. V. Lomakov, Science Research Institute of Physics at the Rostov-na-Donu State University]

[Abstract] Experimental observation of collective excitation spectrum in the planar 2*D* phase of superfluid ^{3}He are reported and the spectrum is investigated by the path integration method developed for this purpose by Brusov and Popov. The spectrum is found to contain both the modes already known from the *A*-phase, i.e., the goldstone, the clapping, the pairbreaking, and new modes which exist solely in the 2*D* phase. These modes were obtained in a magnetic field and their frequencies are close to each other and depend on the field. On the other hand, the frequencies of the clapping and pairbreaking modes exhibiting Zeeman's linear effect in the *A*-phase do not depend on the magnetic field in the 2*D* phase. The collective modes have a complex energy due to the disappearance of the gap in the single-particle spectrum along a fixed direction; this is also similar to the *A*-phase case. A new mode characteristic only of the 2*D* phase whose energy is somewhat higher than the energy of the superflapping mode at all temperatures is reported; the mode is attributed to spin waves and is neither resonant nor diffuse. The authors are grateful to M. O. Nastenka, T. V. Filatova-Novoselova, V. N. Popov, J. B. Ketterson, Z. Zhao, I. Fomin, Yu. M. Bunkov, Ye. Chervonko, and M. Krusius for discussing the results. Tables 1; references 12: 5 Russian, 7 Western.

Temperature Dependence of Nonlocal Resistance in Quantum Hall Effect Condition

927J0066B Moscow PISMA V ZHURNAL EKSPERIMENTALNOY I TEORETICHESKOY FIZIKI in Russian Vol 53 No 9, May 91 pp 461-465

[Article by V. T. Dolgopolov, A. A. Shashkin, G. M. Gusev, Z. D. Kvon, Solid State Physics Institute at the USSR Academy of Sciences, Chernogolovka, and Semiconductor Physics Institute at the Siberian Department of the USSR Academy of Sciences, Novosibirsk]

[Abstract] The role of edge states in current transport in Hall bridges under the conditions of integral Hall effect and the probable contribution of edge states to current in a dissipative condition manifested by the nonlocal effects observed in samples are discussed. The results of preliminary experiments to observe nonlocal effects, and in particular, the temperature dependence of nonlocal

resistance in a single AlGaAs/GaAs heterojunction with an electron concentration of 4.9 x 10^{11} cm^{-2} and a mobility of 60 m^2/V x s are presented. The temperature dependence of nonlocal resistance in the vicinity of the 1.5 filling factor is examined. A comparison of experimental and theoretical data makes it possible to establish the temperature dependence of the frequency of transitions between quantum levels; moreover, the experiments confirm that the equalization length of the edge state and the upper populated Landau level depend on temperature. The observed temperature dependence may be attributed to the process of electron-phonon scattering with a spin reversal near the sample boundary. The authors are grateful to S. I. Dorozhkin, K. A. Matveyev, A. V. Khayetskiy, V. I. Falko, and V. B. Shikin for helpful discussions and remarks. Figures 3; references 17: 1 Russian, 16 Western.

Theory of Energy Relaxation in Two-Dimensional Electron Crystal on Surface of Liquid Helium

927J0068A Kharkov FIZIKA NIZKIKH TEMPERATUR in Russian Vol 17 No 8, Aug 91 pp 933-940

[Article by Yu. P. Monarkha. Institute of Low-Temperature Engineering Physics, UkSSR Academy of Sciences, Kharkov, and V. B. Shikin, Institute of Solid-State Physics, USSR Academy of Sciences, Chernogolovka (Moscow Oblast)]

UDC 532.132

[Abstract] Crystallization of a two-dimensional gas of surface electrons in liquid helium and attendant static deformation of the helium surface underneath a two-dimensional Wigner electron crystal forming are considered, a theory being constructed for an evaluation of the relaxation of electron energy in such a crystal. It is constructed on the premise that scattering of electrons at temperatures below 0.8 K occurs principally in electron-ripplon interaction. It is based on the Hamiltonian of this interaction as a function of surface displacements and, while only its linear terms need to be known for a determination of the electron mobility or for taking static surface strain into account, its quadratic terms are needed for determining the relaxation rate so that also these terms must be known for a correct determination of the energy relaxation time. The problem of electron-electron correlations and energy relaxation reduces then to calculation of the form factor for such a crystal under conditions of strong electron-ripplon interaction and resulting static deformation of the surface relief underneath the crystal. That static deformation is self-consistently taken into account, a Wigner crystal being considered which, as a whole, is at rest. The remarkable feature here is that both the strain distribution over the crystal surface and the threshold frequency of optical modes in the crystal are determined by long-wave ripplons, while mainly short-wave ripplons participate in elementary generation and annihilation events. The energy relaxation time will thus be determined by both the long-wave asymptotic limit for V_q function and the short-wave asymptotic limit for the $W_{q,q'}$ function in the electron-ripplon interaction Hamiltonian, thus quite differently than in the gas dynamics approximation. The contribution of transverse and longitudinal phonons to the total energy relaxation time are evaluated next. The part of the relaxation time relating to longitudinal phonons is found to be almost negligible at usual low electron temperatures and only in the exotic case of an electron temperature much higher than the helium temperature to be comparable with the part of the relaxation time relating to transverse phonons, in which case the crystal may melt. The temperature dependence of the energy relaxation time τ as well as of parameters δ and λ characterizing transverse and longitudinal phonons respectively has been evaluated up to 0.2 K for a two-dimensional Wigner electron crystal with the following parameters: electron concentration $n_0 = 1.02 \times 10^8$ cm^{-2}; potential barrier for electrons at the liquid-He and He-vapor interface V_0 and electron wave function at the liquid-He surface $f_1 z_0$ 0.97 eV and 56.6 $cm^{-1/2}$, 1.0 eV and 59.7 $cm^{-1/2}$, 1 eV and 58.8 $cm^{-1/2}$. The results are compared with available experimental data and the differences are discussed. Figures 3; references 12.

Current-Induced Andreyev States in Superconductor Junctions

927J0068B Kharkov FIZIKA NIZKIKH TEMPERATUR in Russian Vol 17 No 8, Aug 91 pp 961-970

[Article by S. V. Kuplevakhskiy, Kharkov State University imeni A. M. Gorkiy, and I. I. Falko, Kharkov Polytechnic Institute imeni V. I. Lenin]

UDC 538.945

[Abstract] Appearance of bound states in plain tunneling SIS junctions and point junctions with an attendant appearance of a discrete part in the excitation spectrum is predicted on the basis of general relations governing formation of a potential well under conditions of supercurrent flow. First is considered a symmetric pure SIS junction at temperatures slightly below the critical, in which case the dependence of the pairing potential $|\Delta|$ on the distance x from the barrier is described by the B-C-S linear integral equation at distances within the coherence length and by the solution to the Ginzburg-Landau equation at much farther distances. Annihilation of Cooper pairs by the supercurrent occurs also at temperatures far below the critical, a qualitative analysis of this process, indicating that in this case the pairing potential will dip symmetrically near the barrier and the excitation spectrum will acquire at least one more discrete level. The energy of such a level $E_0^{(0)}(\cos\theta,|\varphi|) = \Delta_\infty[1 - P(\cos\theta)\sin^2\varphi/2]^{1/2}$ (θ - angle of electron incidence on barrier, φ - difference between phases of order parameter), where the probability of tunneling P is a function of $\cos\theta$, is calculated on the basis of the Andreyev states

theory and the two Bogolyubov-de Gennes equations ignoring spin: one for $E\psi$ containing the three Pauli matrices τ_i (i = 1,2,3) in the Gorkov-Nambu space, with the order parameter ψ = (u,v), and one for $\Delta(x)$. It is calculated for that classical symmetric SIS Josephson junction (small phase difference φ) and then also for a symmetric point junction. Inasmuch as the effect of a pairing potential perturbation in a symmetric SIS junction is appreciable, except when the probability of tunneling of normally incident electrons is $P(\cos\theta = 1) << 1$ and thus very low, only the first term of the series expansion needs to be retained so that in the zeroth approximation $E_0(\cos\theta,|\varphi|) = \Delta_\infty[1 - (1/2)P(\cos\theta)\sin^2\varphi/2]$ in the zeroth approximation. Corrections are then made for non-self-consistency. In point junctions is considered the limiting case of a perfect opening for electrons, namely $P(\cos\theta) = 1$ and $E_0 = \Delta_\infty\cos\varphi/2$ ($|\varphi| < \pi$). The theory of Andreyev states is then extended to asymmetric S_1NS_2 junctions (large phase difference φ), subscript ∞ and superscript (0) being omitted and the Bogolyubov-de Gennes equation for $E\psi$ in the zeroth approximation being reformulated so as to account for two energy gaps Δ_1,Δ_2. This equation is solved for $\psi(x)$, assuming for specificity that $\Delta_1 \leq \Delta_2$ and $0 < E \leq \Delta_1$, whereupon a general expression is obtained for $E_0(\cos\theta,|\varphi|)$. Again are considered the limiting cases of a perfect opening for electron tunneling P = 1 and a very low probability of electron tunneling $P << 1$, with appropriate corrections for non-self-consistency. The discrete excitation spectrum in such an asymmetric junction is analyzed, assuming that the three metals differ only in the magnitude of the electron-electron interaction parameter. The authors thank M. A. Obolenskiy for helpful discussion. References 15.

Transfer of Intense Laser Radiation in Optical Media: "Optical Turbulence"

927J0048A Minsk INZHENERNO-FIZICHESKIY ZHURNAL in Russian Vol 61 No 1, Jul 91 pp 21-25

[Article by I. B. Krasnyuk, T. T. Riskiyev, and T. P. Salikhov, Institute of Engineering Physics imeni S. V. Starodubtsev, UzSSR Academy of Sciences, Tashkent]

UDC 621.373

[Abstract] Propagation of laser (monochromatic) radiation through a plane layer of a diathermanous optical medium with diffusely emitting radiation and specularly reflecting opaque surfaces is described by a system of two differential equations of kinetics of one-dimensional radiation transfer, one for each of the two surfaces i = 1,2 with the appropriate boundary conditions at each (sum of two terms representing radiation emitted and reflected respectively). These two equations, linear when the incident radiation is weak, become nonlinear when it is strong and the optical properties of the surfaces ($\varepsilon_{i,\lambda}$) - emissivity for given radiation wavelength, n_λ - refractive index for given wavelength λ, depend on its intensity. These two differential equations are convertible into a single difference equation with continuity in time and appropriate initial condition (I_0 - initial intensity). The behavior of its solutions as time $t \rightarrow \infty$ indicates that the radiation transfer, depending on the value of the parameter $\mu = \varepsilon_{i,\lambda} n_\lambda {}^2I_0(\lambda,T)$ (i = 1,2; T - temperature), either asymptotically relaxes into a steady state or asymptotically approaches a periodically oscillating piecewise-constant preturbulence state. The frequency of oscillations in this case either remains constant in time or increases infinitely according to a power law. The number of discontinuities of the limit function characterizing this state is finite in the first case and is countable infinite or uncountable infinite when that frequency is in the latter case. It is uncountable infinite for a certain existing set of μ values in R^1-space and forms a homeomorphic Cantor set, the number of oscillations within a given time interval is then exponentially increasing ("optical turbulence") as the beginning of this interval $t_0 \rightarrow \infty$. In this case bifurcation of the solutions to that difference equation is accompanied by a change of the periods of oscillations of the optical parameters. Figures 5; references 5.

Coherent Interaction of Phase-Modulated Light Pulses and Active Medium of Two-Level Particles With Attendant Line Broadening

927J0056C Moscow ZHURNAL EKSPERIMENTALNOY I TEORETICHESKOY FIZIKI in Russian Vol 100 No 1(7), Jul 91 pp 105-112

[Article by E. M. Belenov, P. G. Kryukov, A. V. Nazarkin, and I. P. Prokopovich, Institute of Physics imeni P. N. Lebedev, USSR Academy of Sciences]

[Abstract] The problem of producing strong ultrashort laser pulses is considered, amplification of femtosecond pulses occurring either in a medium with a nonuniformly broadened line or in a medium with properties close to those of a nonuniform of ensemble radiators. Femtosecond pulses of ultraviolet radiation are produced by doubling the frequency of light pulses emitted by a dye laser and then amplifying the thus extracted second-harmonic pulses with an excimer laser, the width of the amplification line and the duration of the pulses being such that coherent pulse propagation becomes significant. Femtosecond pulses of near-infrared radiation are produced by prior phase modulation of the pulse carrier and stretching of the pulse, thus the "chirped" pulse then being amplified by passage through an artificial medium where the dispersion of the group velocity is such that pulse compression occurs. In connection with this problem is considered the effect of coherence in a medium consisting of two-level particles where nonuniform broadening of the amplification line occurs while the duration of the pulse becomes shorter than the time taken by nonuniform dephasing of radiation emitting particles. Inasmuch as this requires a rather long interaction space in such a medium when the duration of the entering pulse is much longer than that dephasing time T_2^* but remains shorter than the time T_2 taken by irreversible polarization relaxation in the medium, the practical problem is to minimize this length by shaping the pulse field so that the entire energy stored in the medium will be utilized for amplification of the pulse. Feasibility of this scheme is demonstrated by treating interaction of two-level particles with the field of a phase-modulated pulse as an analog of Landau-Zener predissociation of a diatomic molecule and calculating the efficiency of energy extraction from the medium for amplification of the pulse on this basis. The efficiency η of this process is found to depend principally on the phase of the pulse rather than on its amplitude, transition of particles covering the entire range dephasing time T_2^* ($1/T_2^*$ spectrum) from the upper level to the lower level and utilization of all stored energy ($\eta \rightarrow 1$) thus being attainable by phase modulation of the pulse carrier when the intensity of the pulse field exceeds some critical level. Figures 2; references 16.

Initiation of Warmup Wave in Mixtures and Chemical Compounds Containing Deuterium and Tritium

927J0056D Moscow ZHURNAL EKSPERIMENTALNOY I TEORETICHESKOY FIZIKI in Russian Vol 100 No 1(7), Jul 91 pp 173-188

[Article by I. V. Sokolov, Institute of General Physics, USSR Academy of Sciences]

[Abstract] Generation of plane "combustion" waves in plasmas of deuterium-tritium (D-T) mixtures and compounds with other chemical elements is analyzed in connection with plasma ignition and inertial control of fusion, considering that in most cases only a small inner region of such a plasma is heated by the driver up to the

fusion temperature and its much larger outer region is then heated up by the "combustion" wave emanating from the inner region. Even a small amount of an additive in the outer region impedes the ignition but also influences the "combustion" process and could favorably influence the dynamics of target compression, as long as it does not impede ignition too much. A stationary completely ionized and optically transparent plasma with a constant total ion concentration $n = n_D + n_T + n_a$ ($n_D = n_T$, $a = 2n_D/n$) is considered from which neutrons and radiation can escape freely. Relaxation of thermonuclear α-particles and radiative losses are accounted for in the one-temperature approximation, and all reactions except the D + T reaction are ignored. The conditions for generation of one-dimensional "combustion" waves in such a plasma are established on the basis of the one-dimensional equation of heat conduction by moving α-particles, a plasma where E = 3.5 MeV α particles move at temperatures $T << 100$ keV being still regarded as a stationary one with friction against electrons, the only force acting on such an α-particle. A theoretical analysis and numerical calculations reveal that transport of α-particles plays the dominant role in ignition of an optically transparent plasma occurring in its hotter region where $EJ > Q_r$ at temperatures $T > 5$ keV, (EJ - released energy, Q_r - bulk power of radiative losses), while electrons carry heat in the cold region where $EJ < Q_r$. The criterion of formation of a warmup wave in a Lorentz plasma for ignition of such a plasma is then established on the basis of the applicable integrodifferential transient-state energy equation, considering that linear temperature perturbations in a cold (T = 0 keV) plasma will decay while localized temperature perturbations of a finite amplitude such that $EJ > Q_r$ at the peak temperature can increase, but only when they extend over a sufficiently large distance. There naturally exists an intermediate state between increasing and decreasing temperature perturbations, this state being described by the steady-state solution to that energy equation which in turn satisfies the corresponding integrodifferential steady-state energy equation. Heat conduction by electrons is found to be negligible when the mean-squared charge number $z^2 >> 3$, this condition being satisfied at temperatures $T > 8$ keV. The parameters of threshold steady-state excitation such as $b = (C/C_e)/(EJ/Q_r)$ (C - total thermal conductance, C_e - electronic thermal conductance) and the temperature-dependent integral $I(T) = [C(1 + Q_r/EJ)\delta T/\delta x]^2/2$ ($\delta T/\delta x$ - longitudinal temperature gradient) are then calculated, heat conduction by electrons not being negligible when the mean charge number z and mean-squared z^2 are small. Inasmuch as steady-state solutions to that energy equation have meaning here only when they are unstable, of further concern are the rate of perturbation buildup and the transient temperature rise after the ignition criterion has been exceeded and $EJ >> Q_r$. The rate of perturbation buildup $\delta T/\delta t$ is obtained from the equation analogous to the transient-state energy equation after the integral operator has been replaced with the differential one, really unstable at all values of the parameter $S = (\text{mean } z)(\text{mean } z^2)/a^2$. On this basis is then also calculated the rate of increase of the perturbation length $V \approx d\Delta x/dt$. Evolution of the longitudinal temperature profile T(x) is evaluated for S within the $S_c < S < S_0$ range (S = 28.5 for the solid $LiBD_4 + LiB_T$ compound) and for S within the $1 < S_c < S_c$ range ($S_0 \approx 33$ and $S_c \approx 27$ being respectively the upper and lower limits of the range of existence of a steady-state solution to that steady-state energy equation). The author thanks S. V. Bulanov and Yankov for discussing the results, also P. V. Sasorov for helpful consultations. Figures 3; references 27.

Numerical Simulation of Electron-Beam-Pumped XeF(B-X)-Laser Emission Spectrum

927J0059A Moscow KVANTOVAYA ELEKTRONIKA in Russian Vol 18 No 7(229), Jul 91 pp 785-790

[Article by A. V. Abarenov, I. G. Persiantsev, A. T. Rakhimov, S. P. Rebrik, N. V. Suyetin, Yu. S. Shugay, Nuclear Physics Scientific Research Institute at the Moscow State University imeni M. V. Lomonosov]

UDC 621.373.826.038.823

[Abstract] The features of XeF(*B-X*)-lasers which distinguish them from other inert gas halide lasers, primarily their complex stimulated emission spectrum containing lines corresponding to partially overlapping 0-3, 1-4, 0-2, and 1-6 electron-vibrational transitions, are discussed and the need to develop a computer model which would reflect basic characteristics of real systems and describe in principle the dependence of the electron-beam-pumped XeF laser's stimulated emission spectrum on the pump power and temperature is identified. A model of an electron-beam-pumped XeF(*B-X*)-laser is produced; the behavior of the emission power in various spectral bands is simulated allowing for the finite rotational relaxation time and is consistent with experimental data; weak signal gain is also consistent with experimental data. The dependence of integral emission spectra on the working medium temperature and pump power is found; the laser system efficiency (KPD) is also consistent with the experiment. An increase in the XeF(*B-X*)-laser efficiency with temperature is attributed to a redistribution of vibrational *X*-state populations and a stimulated emission enhancement in the spectrally overlapping 1-4 and 0-2 electron-vibrational transitions. The best consistency of analytical and experimental data is attained if the stimulated emission cross-sections (SVI) in the 351 nm band is reduced by a half, probably due to the failure to take into account narrow-band absorption in this region. Figures 8; tables 2; references 24: 2 Russian, 22 Western.

Optical Klystron's Spatial Radiation Structure

927J0059B Moscow KVANTOVAYA ELEKTRONIKA in Russian Vol 18 No 7(229), Jul 91 pp 795-798

[Article by A. A. Andreyev, V. I. Zhulin, A. P. Mikhaylovskiy, K. Yu. Platonov, State Optics Institute imeni S. I. Vavilov, Leningrad]

UDC 621.373.826

[Abstract] Recent interest in free-electron lasers (LSE) is discussed and a free-electron laser design, referred to as an optical klystron (OK), which has certain advantages over traditional free-electron lasers, e.g., a higher gain, is considered. The optical klystron's optical train consists of a stable double-mirror resonator containing two wigglers with a special device which increases the electron bunching. An equation is derived which describes the spatial structure of optical klystron radiation. The optical klystron's transverse field structure is examined using a special IBM PC program which was developed allowing for nonlocal saturation. An analysis shows that the above nonlocal saturation model does not lead to a principal difference from local saturation. It is established that stable eigenmodes whose structure depends little on the gain saturation model may exist in the optical klystron resonator. At low Fresnel numbers, the emission beam divergence is primarily determined by the resonator's optical train. The authors are grateful to N. A. Vinokurov and V. Ye. Semenov for helpful discussions. Figures 4; references 6: 4 Russian, 2 Western.

High-Efficiency YSGG:Cr, Nd-Laser With Polarizationally-Closed Resonator

927J0059C Moscow KVANTOVAYA ELEKTRONIKA in Russian Vol 18 No 7(229), Jul 91 pp 805-807

[Article by G. I. Dyakonov, V. G. Lyan, V. A. Mikhaylov, S. K. Pak, I. A. Shcherbakov, General Physics Institute at the USSR Academy of Sciences, Moscow]

UDC 621.373.826.038.825.2

[Abstract] The need to eliminate the detrimental effect of thermal birefringence on the output characteristics of solid-state lasers emitting trains of linearly polarized monopulses at repetition frequency is identified and it is suggested that polarizationally closed resonators (PZR) be used in YAG:Nd lasers for this purpose. The use of such resonators is especially efficient in YSGG:Cr, Nd-lasers in which the high level of thermal birefringence makes it difficult to realize the high gain potential even at a low pump power. An almost 3.1 percent efficiency is attained in an electrooptically Q-switched YSGG:Cr, Nd-laser with a polarizationally closed resonator, given a linearly polarized output monopulse power of up to 0.4 J. The laser's output parameters are virtually independent of the thermal birefringence level in the active element at a pulse repetition rate of up to 50 Hz. The use of these resonators in lasers on the basis of materials with relatively high thermal optical distortions, such as scandium garnets, various types of glass, etc., appears promising. Figures 3; references 4.

Spectrum Compression of Ultrashort Laser Pulses

927J0059D Moscow KVANTOVAYA ELEKTRONIKA in Russian Vol 18 No 7(229), Jul 91 pp 865-867

[Article by N. L. Markaryan, L. Kh. Muradyan, T. A. Papazyan, Lazernaya Tekhnika Scientific Production Association at the Yerevan State University]

UDC 621.373.826

[Abstract] The importance of fiber optic compression (VOK) technology for mastering the femto- and picosecond range of ultrashort laser pulses (UKI) prompted by the onset of ultrafast process spectroscopy and the need to attain extremely short durations and control the spectrum, time envelope, and certain statistical parameters of ultrashort laser pulses is discussed. In so doing, the possibility of developing an ultrashort laser pulse spectrum compression system on the basis of fiber optic compression devices is studied analytically and numerically. Fiber optic compression principles are based on the pulse's phase self-modulation in a single-mode optical fiber (OVS) and its subsequent compression in a dispersion delay line (DLZ); a pair of a diffraction grating can be conveniently used for the latter purpose. A mathematical description of both processes is given. It is shown that a diffraction grating-optical fiber system can be used for compressing the ultrashort laser pulse spectrum and basic relationships which make it possible to optimize a spectral compressor are derived. Since ultrashort pulses of real laser sources are randomly modulated to a certain extent, the use of the proposed system for suppressing the laser noise, i.e., extracting the regular emission component, appears promising. Figures 3; references 7: 4 Russian, 3 Western.

Interaction of Square Neodymium Laser Radiation Pulse With Metals

927J0059E Moscow KVANTOVAYA ELEKTRONIKA in Russian Vol 18 No 7(229), Jul 91 pp 872-876

[Article by V. K. Goncharov, V. I. Karaban, V. L. Kontsevoy, T. V. Stasyulevich, Scientific Research Institute of Applied Physics Problems imeni A. N. Sevchenko at the Belarus State University imeni V. I. Lenin, Minsk]

UDC 621.373.826:533.9

[Abstract] The interaction of neodymium laser radiation pulses with various metals whereby a finely dispersed liquid drop phase of the target materials enters the erosion flame (EF) and absorbs and scatters laser radiation in the free lasing operation (RSG) which is characterized by a chaotic distribution of the laser emission power density in time and space is discussed. Zinc, cadmium, lead, and tin targets were irradiated by close to square neodymium laser pulses. The results of experimental spectroscopic measurements of the resulting erosion flame are cited; the behavior of the probing radiation absorption and scattering coefficients during

the exposure is plotted. The power density ranges within which the liquid drop phase noticeably affects the optical characteristics of the laser's erosion flame are found for the above metals. The study confirms that metal breakdown under the effect of laser radiation in the free lasing operation or square pulses is principally similar; only a quantitative difference is observed. The authors are grateful to Yu. A. Stankevich and A. S. Smetannikov for useful discussions. Figures 6; references 22.

Wide-Aperture X-Ray Source for Preionization of High-Volume Electric-Discharge Lasers

927J0059F Moscow KVANTOVAYA ELEKTRONIKA in Russian Vol 18 No 7(229), Jul 91 pp 891-893

[Article by S. N. Buranov, V. V. Gorokhov, V. I. Karelin, A. I. Pavlovskiy, P. B. Repin, All-Union Scientific Research Institute of Experimental Physics, Arzamas, Nizhniy Novgorod oblast]

UDC 621.373.826.038.823

[Abstract] The problem of preionizing the active medium in large-scale lasers, especially excimer lasers where increasingly stringent requirements are imposed on the initial electron concentration and uniformity in the active volume, is discussed. The role of X-ray sources in developing the initial plasma in electric-discharge plasma on the basis of three-electrode pumping discharge generating structure (TSF) is investigated in CO_2 laser units with a 12 l active volume and 9.7 cm electrode gap. The study shows that the high-voltage diffuse atmospheric pressure discharge in the electric discharge structure formed by a system of wires and a planar mesh serves as a highly efficient X-ray source for preionizing the active medium. Given a 40x200 cm source aperture, the X-ray dose provided in the active medium of electric-discharge CO_2 lasers with an up to 0.28 m^3 volume exceeded 60-300 R. There are no physical constraints for increasing the nanosecond X-ray source aperture. This makes three-electrode structures promising for designing and developing large-scale electric-discharge lasers. Figures 3; references 13: 12 Russian, 1 Western.

Anomalous Radiation Absorption by Ammonia in Strong Laser Field

927J0069A Moscow PISMA V ZHURNAL EKSPERIMENTALNOY I TEORETICHESKOY FIZIKI in Russian Vol 54 No 3, 10 Aug 91 pp 138-142

[Article by V. N. Lokhman, G. N. Makarov, and V. M. Sotinkov, Institute of Spectroscopy, USSR Academy of Sciences, Troitsk (Moscow Oblast)]

[Abstract] An experimental study was made in search of answers concerning excitation of molecules from many rotational states, namely whether the excitation efficiency depends on the pump being at or off resonance with any of the transitions in such a molecule and whether depletion of many rotational states takes place upon excitation of simple molecules where multiphoton processes at the lower levels are not likely to take place in an infrared radiation field of moderate intensity. For the test case an ammonia molecule had been selected, characterized not only by a high spectral resolution of vibrational-rotational transitions facilitating excitation at resonance or off resonance with individual transitions but also by highly anharmonic vibrations due to inversion splitting of ν_2-mode excitation levels ($\Delta\nu_{anh} \approx 300$ cm^{-1} at 1a $\rightarrow$ 2s transition) in an infrared laser field of moderate 10^5 - 10^7 W/cm^2 intensity. A transverse-excitation atmospheric-pressure CO_2-laser emitting 9R(30)-line radiation of $I \geq 10^6$ W/cm^2 intensity was used for pumping these molecules in pulses of a duration τ_p much shorter than their rotational-states relaxation time τ_r so as to ensure a collisionless process with $p\tau << p\tau_r = 50$ ns (p - ammonia pressure) in the first excited vibrational state. The absorption of radiation energy by NH_3 molecules was measured with a pyroelectric transducer and a calorimeter. The percentage brightening of transitions in NH_3 molecules other than those excited at or off resonance was determined on the basis of measurements made by the double infrared resonance method in terms of the $\eta = (\sigma_0 - \sigma_e)/\sigma_0$ ratio (σ_0 and σ_e denoting the cross-sections for absorption of probing radiation by NH_3 molecules without and after prior excitation respectively), this method involving use of two identical CO_2-lasers and two pyroelectric transducers with the time difference τ_d between exciting pulse and delayed probing pulse sufficiently small to make $p\tau_d << p\tau_r$. More sensitive and accurate measurements were made by the optoacoustic method under conditions of double infrared resonance, letting the optoacoustic signal form within a time $\tau_{OA} \geq 100\ \mu s\ \tau_d$. The data have been analyzed for dependence of energy absorption by NH_3 molecules (average number of energy quanta per molecule) during their sR(5,k) transition on both the ammonia pressure over the 0.01-1.0 torr range and on the surface density of pumping energy over the 0.1-10 J/cm^2 range, also for energy density and pressure dependence of the sQ(2,K)-transition brightening during sR(5,K) transition pumping and of the sR(5,K)-transition brightening during sQ(2,K)-transition pumping. The results demonstrate that radiative excitation of molecules from many rotational states takes place during pumping of their one-photon transitions by intense infrared radiation and that their other rotational states are then depleted with an efficiency much higher during resonant pumping than during off-resonance pumping. The difference cannot, however, be adequately explained in terms of multiphoton transitions. The authors thank A. A. Makarov for fruitful discussion of the results and for valuable comments. Figures 3; references 11.

Shaking Mechanical Microparticles Off Silicon Surface With Acoustic Wave Generated by Laser Pulse

927J0071C Leningrad PISMA V ZHURNAL TEKHNICHESKOY FIZIKI in Russian Vol 17 No 13, 12 Jul 91 pp 62-66

[Article by A. A. Kolomenskiy and A. A. Maznev, Institute of General Physics, USSR Academy, Moscow]

[Abstract] Cleaning solid surfaces from solid microparticles in the micron and submicron size ranges by surface acoustic waves (SAW) generated by laser pulses acting on the surface was demonstrated in an experiment with wafers cut from a silicon single crystal, the aim being to attain local acceleration forces sufficiently high to overcome adhesion and cause breakaway of dust. Wafers of KEF4.5(100) silicon, 380 μm thick and 76 mm in diameter, were covered with alumina dust and placed vertically in a test chamber. Radiation pulses of 10 mJ energy and 10 ns duration emitted by a YAG:Nd^{3+}-laser in the TEM_{00} mode were focused by a cylindrical lens on a 3 mm wide and 10 μm thick wafer surface strip running in the [110]-direction. The surface was probed with a He-Ne laser beam, SAW pulses generated upon optical breakdown deflecting this beam. The angle of surface inclination in a surface acoustic wave was recorded in this way and found to be proportional to the normal component of the vibrational velocity of the surface. Tests were performed with the chamber containing air under atmospheric or vacuum with a residual pressure of 0.1 torr. The cleaning mechanism is analyzed theoretically in terms of forces acting on a microparticle under these conditions, using the Gamacker relation for a Van der Waals adhesion force. The normal surface acceleration necessary for the breakaway force to exceed such an adhesion force is calculated accordingly and found to be larger for smaller particles. Removal of particles is more difficult in air than under vacuum, apparently because of their redeposition on the surface by the opposing drag force. For a 0.4 μm or larger size particle of a material which has a density of 4 g/cm^3 the calculated threshold acceleration is 190 km/s^2 under vacuum. The experimental data agree closely with the theoretical ones. The method is recommended for cleaning semiconductor wafers in production of integrated circuits, for contactless measurement of adhesion forces acting on extremely fine particles, and for visual display of propagating SAW pulses. The authors thank Yu. N. Petrov for very stimulating discussions, also Yu. V. Panfilov, D. O. Boykov, and R. A. Karabanova for assistance. Figures 3; references 7.

Characteristics and Expansion Dynamics of Erosion Plasma Formed by XeCl Laser's Ultraviolet Radiation

927J0075A Moscow FIZIKA PLAZMY in Russian Vol 17 No 8, Aug 91 pp 918-923

[Article by D. V. Gaydarenko, A. G. Leonov, D. I. Grekhov, Moscow Engineering Physics Institute]

UDC 533.9:621.375.826

[Abstract] The importance of understanding the characteristics and expansion dynamics of the erosion plasma formed under the effect of laser radiation on the target surface for various applications, such as deposition of thin films and development of ion sources, and the role of plasma forming threshold, the dependence of plasma density and temperature on distance, the velocity, energy, and directional pattern of the plasma scattering, etc., are discussed. An attempt is made to examine and classify the erosion flame developing on the surface of aluminum under the effect of ultraviolet (UV) radiation of a XeCl excimer laser with a close to 100-1,000 MW/cm^2 intensity in order to determine the plasma parameters and their space time dependence. An electric-discharge-pumped laser with a pulse energy of up to 0.5 J and a half-height pulse duration of close to 20 ns is used in the study in which the interaction of this laser's ultraviolet radiation at a 308 nm wavelength with the aluminum surface in a close to 10^{-5} torr vacuum is examined experimentally. The erosion flame plasma density and temperature as a function of time, coordinate, and intensity are measured by the spectral and probing methods. The results are used to trace the principal patterns of the plasma cloud expansion, making it possible to speculate that breakdown on the surface is resonant because the laser wavelength and the $^2P_{1/2}$ - $^2D_{3/2}$ transition wavelength coincide in the aluminum atom. A photodetector on the basis of a charge-coupled device (PZS) array is used to measure the laser radiation profile in the focusing region. The authors are grateful to I. V. Novobrantsev for constant attention in the effort and a useful discussion of the findings and A. V. Brazhnikov for help with the experiments. Figures 4; references 17: 9 Russian, 8 Western.

Amplification of High-Frequency Pulse Trains in Neodymium Glass Laser Systems

927J0077D Leningrad ZHURNAL TEKHNICHESKOY FIZIKI in Russian Vol 61 No 4, Apr 91 pp 99-104

[Article by T. A. Murina, V. A. Rusov]

[Abstract] The need for light sources producing trains of high-power pulses at a repetition rate of tens and hundreds of kilohertz with a stable amplitude within the train in various information systems, e.g., ranging and locating, communications, photographic, etc., is identified. The stability of a high-frequency pulse train generated in a neodymium glass laser system is investigated theoretically and experimentally. In so doing, the conditions necessary for producing a train of equal-intensity pulses are analyzed. The problem is solved on the basis of the point mapping method, used before for a generator producing a high-frequency pulse train, in the framework of the Franz-Nodvik model. Lamerey's amplification condition diagrams which explain the periodic stimulated emission intensity dynamics are cited and the stable operation realization conditions are determined. The laser system used in the experiment consists of a master oscillator (the neodymium glass laser), a preamplifier, and a two-stage amplifier. It is shown that Lamerey's diagram method makes it possible to solve the problem of studying the stability of pulse trains obtained in laser amplifiers with a two-pass phase conjugation (OVF) stimulated Brillouin scattering (VRMB) mirror design. Figures 5; references 12: 10 Russian, 2 Western.

Ionization (Streamer) Wave Propagation in Air Channel Initiated by Ultraviolet Laser Radiation

927J0077F Leningrad ZHURNAL TEKHNICHESKOY FIZIKI in Russian Vol 61 No 4, Apr 91 pp 200-207

[Article by A. A. Antipov, A. Z. Grasyuk, A. K. Zhigalkin, L. L. Losev, V. I. Soskov, Physics Institute imeni P. N. Lebedev at the USSR Academy of Sciences, Moscow]

[Abstract] Known methods of controlling the spark discharge with the help of laser radiation by creating a highly conducting plasma formation in the electrode gap are discussed and it is noted that they require a high laser emission power and a characteristic laser radiation energy of 10^2 to 10^3 J with a stimulated emission pulse duration of close to 100 ns as well as a rather complicated specially designed optical train. A spark discharge control method which calls for a much lower laser radiation energy due to initiating an electric discharge in a gas channel which is ionized beforehand by ultraviolet (UV) laser radiation is proposed. The possibility of developing an ionization wave—the so-called streamer—propagating in the air through a channel ionized beforehand by ultraviolet laser radiation is investigated. An Nd:YAG mode-locked laser is used as an ultraviolet radiation source. The study demonstrates that propagation of the ionization wave in an ionic channel created in the air as a result of multiphoton ionization by ultraviolet laser radiation is indeed possible. An approximately 35 ps long, 8 mJ laser pulse on a 266 nm wavelength is thus used to control the spark breakdown with a 40 cm long discharge at an approximately 300 kV potential difference. Figures 5; references 9: 7 Russian, 2 Western.

Interaction of Massive Neutrinos With Field of Plane Wave

927J0056B Moscow ZHURNAL EKSPERIMENTALNOY I TEORETICHESKOY FIZIKI in Russian Vol 100 No 1(7), Jul 91 pp 75-81

[Article by V. V. Skobolev, Moscow State Pedagogical Correspondence Institute]

[Abstract] Photoproduction of massive neutrino-antineutrino pairs in the $\gamma \rightarrow \nu\nu$[dash over ν] process and bremsstrahlung emission in the $\nu \rightarrow \nu\gamma$ process are analyzed with the aid of the generalized Dirac equation for a neutral particle with an anomalous magnetic moment μ_ν and an electric dipole moment ε_ν in the field of a plane radiation wave. Invariant solutions to this equation are obtained for a linearly polarized plane wave of the A = af[(kx)] form and for a circularly polarized one. The effective vertex of $\gamma\nu\nu$[dash over ν] interaction induced by μ,ε coupling to the radiation field $A^{(gg)}$ and the matrix element of the $\gamma \rightarrow \nu\nu$[dash over ν] process obtained from the wave function of a neutrino are used for calculating the probability per unit time of $\gamma\nu\nu$[dash over ν]-interaction in the field of a linearly polarized plane radiation wave. A reaction threshold is shown to exist in the special case of a constant crossed field. The probability per unit time of $\nu\nu\gamma$-interaction is calculated analogously, with the neutrino momentum replacing the photon momentum and with the appropriate formulation of the probability integral. Because the integral probabilities here include moments μ and ε in the symmetric combination $\mu^2 + \varepsilon^2$, it is not possible to determine their relative magntitudes in a corresponding experiment. The results of this analysis indicate that, even with the most optimistic estimates of neutrino mass and moments, the characteristics of existing laser fields and known astrophysical fields evidently do not provide sufficient information for identification of the form factors of electromagnetic fields and CP-symmetry breaking in neutrino experiments involving those two interaction channels. References 13.

Structural Transformations in Planar Nematic Liquid Crystals in Ultrasonic Field

927J0056E Moscow ZHURNAL EKSPERIMENTALNOY I TEORETICHESKOY FIZIKI in Russian Vol 100 No 1(7) Jul 91 pp 197-204

[Article by D. I. Anikayev, O. A. Kapustina, and V. N. Lupanov, Institute of Acoustics imeni N. N. Andreyev, USSR Academy of Sciences]

[Abstract] An experimental study of nematic liquid crystals with a planar orientation of molecules was made concerning formation of structures and structural transformations in an acoustic field at ultrasonic frequencies. The results are interpreted on the basis of Kozhevnikov's theoretical model (Ye. N. Kozhevnikov, 1988): 1) a random strain nonuniformly distributed along the crystal layer, attending reorientation of the molecules into positions at angles $\theta = \theta_0(x,z)$ to the plane of that layer, and crystal compression in a normally incident ultrasonic wave give rise to anisotropic shearing stresses $\sigma_{xz} = \theta(\mu_3 v_{zz} + \Delta E u_{zz})$ (x - direction of crystal axis, z - direction of ultrasonic wave, u_{zz} - compressive strain in ultrasonic wave, v_{zz} - compression rate in ultrasonic wave, θ_0 - amplitude of molecule orientation angle relative to crystal plane, $\mu_3(\omega,\tau_1,\tau_2) + i\Delta E(\omega,\tau_1,\tau_2$ - complex modulus of elasticity, τ_1 - relaxation time for order parameter, τ_2 - relaxation time for end groups of molecules, ω - radian frequency of ultrasonic wave); 2) these stresses "develop" oscillating vortices periodically spaced along the crystal layer and moving across it at a velocity v_z' proportional to $\omega_0\cos(qx)$ (q - wave number characterizing periodicity of the longitudinal molecule orientation profile in the crystal layer); 3) interaction of these vortices and the acoustic field produces stationary shearing stresses averaged over the period. According to this model, two mechanisms are operating here: a) convective interaction of vortices and oscillatory motion of the nematic liquid in the acoustic field; b) periodic variation of the viscosity during compression in the ultrasonic wave, which breaks the symmetry of the oscillating vortices. Stationary stresses "develop" in the crystal layer steady vortices moving at a velocity which varies along that layer with the same space period as does the velocity of oscillating vortices. When the incident ultrasonic wave crosses the crystal layer and is reflected by the surface of an acoustically rigid substrate, then a standing wave with a vibration velocity $V_z = 2V_0\sin(kz)\cos(\omega t)$ will form in that crystal layer (V_0-amplitude of vibration velocity of incident wave). The model is valid for ultrasonic frequencies f within the $2\pi\eta/\rho d^2 << f << 2\pi c/d$ range (η - viscosity of nematic liquid, ρ - density of nematic liquid, d - thickness of liquid crystal layer, speed of sound in crystal). Experiments were performed with a eutectic MBBA+EBBA mixture filling a planar capillary channel between a 2 mm thick acoustically rigid glass plate and a thin acoustically soft polymer film with a light-reflecting aluminum coating. The thickness of that capillary channel and of the crystal layer filling it was varied over the 10-360 μm range. In one series of tests the glass plate with the nematic liquid crystal was immersed in water and its distance from the ultrasound radiator varied up to $0.75R^2/\lambda$ (R - radius of radiator, λ - wavelength of emitted ultrasound). In another series of tests a Straubel ultrasound radiator was used producing, through a layer of adhesive on the polymer film, a quasi-uniform wave field in the crystal. The frequency of ultrasound was varied over the 0.3-3 MHz range. The action of ultrasound on the crystal was regulated by varying the voltage applied to the radiator-transducer and was monitored by measuring the intensity of incident ultrasound at the crystal surface. The temperature of the crystal was varied with thermostatic control over the 22-45°C range. The data indicate that reorientation of molecules in a nematic liquid crystal began when the transducer voltage had been raised above its threshold level, whereupon the space period of the molecule orientation profile gradually decreased to a much smaller one which remained constant as the transducer voltage continued to be

raised. They also reveal a direct proportion between that space period and the thickness of the crystal layer. The space period in a crystal layer of any given thickness at any given transducer voltage remained constant as the ultrasound frequency was varied over the 2-10 MHz range at any given crystal temperature and as the crystal temperature was varied over the 20-40°C range at any given ultrasound frequency, becoming temperature dependent as the temperature was raised further. The reorientation pattern began to become irregular at about 44°C and the new structure vanished altogether at about 49°C. The threshold amplitude V_0* of the vibration velocity has been found to drop somewhat with increasing thickness of the crystal layer and to rise with rising ultrasound frequency. The results of this study corroborate the involvement of a new mechanism here according to Ye. N. Kozhevnikov, namely steady-state structural distortion of planar nematic liquid crystals in a standing ultrasonic wave. The authors thank Ye. N. Kozhevnikov for discussing the results. Figures 3; tables 1; references 13.

Investigation of *p*-Resonance Properties in ^{235}U Fission by 1-136 eV Neutrons

927J0065A Moscow PISMA V ZHURNAL EKSPERIMENTALNOY I TEORETICHESKOY FIZIKI in Russian Vol 54 No 1, July 91 pp 9-12

[Article by A. M. Gagarskiy, S. P. Golosovskaya, A. B. Laptev, G. A. Petrov, A. K. Petukhov, Yu. S. Pleva, V. Ye. Sokolov, O. A. Shcherbakov, Nuclear Physics Institute imeni B. B. Konstantinov at the USSR Academy of Sciences, Gatchina, Leningrad oblast]

[Abstract] Manifestations of the effects of spatial parity loss and the phenomena occurring in the cross-section of neutron *p*-resonances are discussed and a new method of obtaining relevant information is proposed. It amounts to studying the energy dependence of the *P*-even "forth and back" fission fragment asymmetry due to an interference of *s*- and *p*-compound states during the capture of slow neutrons which has a singularity in the vicinity of the *p*-resonance. The study was carried out in a neutron beam in a time-of-flight GNEYS spectrometer within a 1-136 eV energy band using a multisection fast ionization chamber containing about 2 g ^{235}U. Thus, a "forth and back" ^{235}U fission fragment scattering asymmetry relative to the neutron momentum direction is measured and irregularities in the curve of the energy dependence of the skewness coefficient due to the *p*-resonance are discovered. Effective parameters of the strongest *p*-resonances are determined. These data are useful both from the viewpoint of neutron spectroscopy of heavy nuclei and basic research of the *P*- and *T*-invariance loss phenomena. It is anticipated that such studied would be carried out in the future for ^{233}U and ^{239}Pu nuclei. Figures 1; tables 1; references 10: 3 Russian, 7 Western.

On Theoretical Interpretation of Experimental Data on ^{235m}U (76.8 eV) Isomer Excitation in Plasma

927J0066A Moscow PISMA V ZHURNAL EKSPERIMENTALNOY I TEORETICHESKOY FIZIKI in Russian Vol 53 No 9, May 91 pp 441-443

[Article by Ye. V. Tkalya, Institute of Nuclear Power Development Safety at the USSR Academy of Sciences, Moscow]

[Abstract] A successful series of experiments to excite the low-lying ^{235m}U $1/2^+$(76.8 eV) state in plasma formed by an electron beam on the surface of metallic uranium enriched to 99.99 percent and performed in a Triton unit at the Atomic Energy Institute imeni I. V. Kurchatov is described. Inverse internal electron conversion (OVEK) is found to play a dominant role in exciting the nuclei by plasma. An attempt is made to explain the isomer nuclei yield in the experiments; to this end, the isomer production mechanism in the experiment which, to a certain extent, is an alternative to the processes in which plasma plays a key role is considered. The conclusion is drawn that the low-lying isomer production in plasma created by an electron beam is probably due to the excitation of higher-lying states as a result of the inelastic electron scattering in the beam by the uranium nuclei. It is stressed that with respect to the foregoing, high-current accelerators used for creating hot plasma may serve as a valuable tool for studying low-lying isomer states of nuclei, e.g., ^{201}Hg whose life of the first excited state with a 1.561 keV energy remains unknown. The author is grateful to R. V. Arutyunyan, V. A. Kornilo, and S. A. Dorshakov for helpful discussions. Figures 1; references 10: 9 Russian, 1 Western.

Possible Amplification of Coherent Radiation in Various Subsurface Channeling Schemes

927J0073A Leningrad ZHURNAL TEKHNICHESKOY FIZIKI in Russian Vol 61 No 5, May 91 pp 55-64

[Article by V. L. Vinetskiy (deceased) and M. I. Fayngold, Institute of Physics, UkSSR Academy of Sciences]

[Abstract] Planar channeling of particle beams through a crystal according to two new schemes is considered, both essentially analogous to the Bragg-Darwin scheme in crystal X-ray optics but involving injection through the front face but with a small glancing angle $\theta \approx 0$ of the incident beam so that also the channeling angle is small $\theta_{ch} << 1$. The direction of photon emission during channeling of electrons or positrons makes in the first configuration also a small angle $\delta << 1$ with the direction of channeling rather than a $\delta = \pi/2$ angle in the standard scheme with channeling in the direction normal to the front face or a $\delta = 0$ angle in the scheme with beam injection through a lateral face. Amplification of the characteristic radiation emitted by the particles of an electron or positron beam during their channeling is first analyzed theoretically, taking into account that their radiation pattern is highly anisotropic and that the

condition $\theta_{ch} << \theta << 1$ is easily satisfied. Considering further that the penalty for lengthening the channel and thus increasing the gain is a smaller depth of beam penetration under the crystal surface, constraints on the particle beam are established in terms of maximum allowable angle of beam divergence and width of particle energy spread. In the first scheme the incident particle beam enters the crystal through a front face perpendicular to the reflecting close-packed atomic planes at an angle $\theta << 1$ rather than $\theta \approx \pi/2$. This scheme allows for smooth variation of the frequency by rotation of the crystal. In the second scheme the front face is cut at a small bevel angle δ to the reflecting parallel close-packed atomic planes and the particle beam enters through it normally to those planes, thus making with that face, another small angle θ and with those planes an angle ξ equal to angle ξ_j at which particles become trapped at respective "transverse" energy levels $E_{trans,j}$ (j = 0,1,2,..) in the channel during selective population of these energy levels. Theoretical calculations are supplemented with numerical estimates on channeling 50 MeV relativistic electrons along a (100) plane in silicon and amplified emission of hard photons during stimulated radiative $2 \rightarrow 1$ transition. Figures 5; references 11.

Cylindrical Solitons in Goedel's Universe and Their Stability

927J0074B Tomsk IZVESTIYA VYSSHIKH UCHEBNYKH ZAVEDENIY: FIZIKA in Russian Vol 34 No 5, May 91 pp 24-27

[Article by K. A. Bronnikov, Yu. P. Rybakov, and G. N. Shikin, "Amity of Nations" University imeni Patrice Lumumba]

UDC 530.12

[Abstract] Soliton models of elementary particles with cylindrical symmetry in the simplest "magnetic" gravitational field are constructed, the field having a metric with a nondiagonality not removable by transformations of coordinates, in the rotating field of Goedel's universe with the $ds^2 = dt^2 - d\rho^2 + \Omega^{-2}(\sinh^4\Omega\rho - \sinh^2\Omega\rho)d\varphi^2 - (8^{1/2}/\Psi)\sinh^4\Omega\rho d\varphi dt - dz^2$ metric (ρ - radial coordinate, $\Omega = \omega/2^{1/2}$, ω - speed of rotation). Interaction of the scalar field φ and a vector field $F_{\mu,\nu}$ is described by the corresponding part of the total Lagrangian, its expression in the form $-F^{\alpha\beta}F_{\alpha\beta}\Psi(\varphi)$ ($\Psi \equiv 1$ for a linear mixture of fields) making the unique nontrivial equation for $F_{\mu\nu}$ readily integrable. For the radial field profile $\psi(\rho)$ can then be obtained the equation $2g^{1/2}(g^{1/2}\psi')' = q^2 dP/d\psi$ with "induced nonlinearity" ($P = 1/\Psi$, $g = |\det g_{\mu\nu}| = \Omega^{-2}\sinh^2\rho \cos h^2\Omega\rho$, $q = F^{01}g^{1/2}\Psi = \text{const}$). The soliton solutions to this equation are characterized by regularity throughout space and localization of energy, finite energy density being a good criterion for regularity and the necessary condition for it being that $P(\varphi) \approx (\varphi - \varphi_a)^2$ when $\varphi \approx \varphi_a$ (φ_a - magnitude of φ on the axis $\rho = 0$). When function $P(\varphi)$ satisfies this condition and also $P(\varphi) = \cos^2\lambda\varphi$ ($\lambda = \text{const} > 0$) so that the field equation reduces to one of the sine-Gordon kind, then inclusion of the external gravitational field is shown to "diffuse" the mass spectrum of solitons and in a special case facilitate asymptotic exclusion of the interaction. Another class of solitons will exist when the interaction is such that the solution to the field equation will have a solution which is trivial outside some surface $\rho = \rho_0$. Stability analysis of all these cylindrically symmetric solitons involves the linearized field equation for $\delta\psi = \chi(t,\rho)$ perturbations of the scalar field which do not break that symmetry. Since the Cauchy problem for this equation is ill-conditioned in the Adamar sense in the $g^{00} < 0$ region, only droplet solutions can be stable in the Lyapunov sense when they are localized in the $g^{00} > 0$ region. The boundary condition $\chi(0) = 0$ is necessary for ensuring finiteness of the energy density at $\rho = 0$. References 3.

Fission of ^{238}U Nuclei by 1 GeV Protons Into Three Fragments of Comparable Mass

927J0076A Moscow PISMA V ZHURNAL EKSPERIMENTALNOY I TEORETICHESKOY FIZIKI in Russian Vol 54 No 6, Sep 91 pp 311-314

[Article by A. A. Zhdanov, V. I. Zakharov, A. V. Kravtsov, G. Ye. Solyakin, N. P. Filatov, Leningrad Nuclear Physics Institute imeni B. P. Konstantinov, Gatchina, and Radium Institute imeni V. G. Khlopin, Leningrad]

[Abstract] Deep fission of ^{238}U nuclei into two massive fragments accompanied by the formation of a large number of particles is treated a reaction of fission into three fragments of comparable mass one of which is nuclear-unstable; this reaction is compared to nuclear fission of ^{238}U irradiated by relativistic protons into three detectable fragments of comparable mass. Data obtained in experiments with fission of ^{238}U nuclei by 1 GeV protons are compared from the viewpoint of the probability of the above two processes and scattering kinematics of the resulting massive fragments. Experiments were carried out using proton beams generated by the Gatchina synchrocyclotron with the help of a time-of-flight double-beam spectrometer and 200 μm photoemulsion layers saturated with ^{238}U nuclei; to improve the detectability of three-beam events pertaining to comparable-mass fragments, the photoemulsion layer sensitivity threshold was raised to the ionization loss levels corresponding to charged fragments with $Z = 10$, making it possible to observe up to 100 double fission events in a 180 μm field of view. Fragment scattering kinematics of both processes have much in common; most recorded events are coplanar. The results make it possible to speculate that the third massive nuclear-stable fragment detected in the ^{238}U fission by 1 GeV protons is formed from nuclear-unstable fragments of this nucleus's fission into three fragments of comparable mass. The relative probability of ^{238}U triple fission by 1 GeV protons where one of the comparable-mass fragments is nuclear unstable is $(9+/-2) \times 10^{-3}$ which is almost 20 times higher than that of fission into three detectable fragments. Figures 2; references 6: 3 Russian, 3 Western.

Lens Design for Focusing Hollow Charged Particle Beams

927J0077E Leningrad ZHURNAL TEKHNICHESKOY FIZIKI in Russian Vol 61 No 4, Apr 91 pp 141-147

[Article by L. P. Ovsyannikova, S. V. Pasovets, Ye. V. Shpak, Engineering Physics Institute imeni A. F. Ioffe at the USSR Academy of Sciences, Leningrad]

[Abstract] The use of hollow beams of charged particles in many devices which can be focused by conventional axisymmetric lenses with a covered center or electrostatic coaxial lenses with a radial field is discussed and fields in such electrostatic coaxial lenses are investigated. A model for approximating these fields is suggested and particle trajectories in the lens are analyzed with the help of this model and compared to trajectories in a field obtained analytically by numerical integration of Laplace's equation. Conditions for correcting the chromatic aberration with the help of a magnetic axisymmetric lens are derived in a weak lens approximation. A coaxial lens formed by two coaxial cylinders is used in the experiments and a series arrangement of one coaxial and one axisymmetric lens is used for chromatic aberration correction. An analytical expression is derived for finding the position of the image with corrected longitudinal chromatic aberration. Figures 4; references 8: 3 Russian, 5 Western.

Scattered-Light Scanning Laser Microscopy and Tomography

927J0081A Moscow IZVESTIYA AKADEMII NAUK SSSR: SERIYA FIZICHESKAYA in Russian Vol 55 No 8, Aug 91 pp 1623-1626

[Article by E. I. Rau, K. K. Frolov, Microelectronics Technology Problems Institute at the USSR Academy of Sciences]

UDC 539.25:620.187

[Abstract] The development and applications of scanning laser microscopy and infrared tomography are outlined, the examples of new methods realized in a laser diagnostics system are considered, and possible uses of new conditions for investigating local characteristics of semiconductors are discussed. New physical and engineering designs aimed at investigating local electric and structural characteristics of semiconductor materials and microelectronic devices are proposed. The use of contactless diagnostic methods made it possible to detect the local surface barrier photoelectromotive force. An up to 10 μm resolution is obtained in a 90° scattering condition. The experiments demonstrate the efficiency and validity of the new realizations of low-angle scattered-light microscopy and the principle of cofocal radiation detection in computer-aided tomography in Rayleigh region scattering, making it possible to determine the cluster formation distribution and visualize these defects. An LG-126 laser and an IBM PC/AT computer are used in the experiments. Figures 3; tables 1; references 9: 5 Russian, 4 Western.

Effect of Preparation Conditions on Au Particle Habitus and Orientation on NaCl Single Crystal (001) Spalling

927J0082A Kiev UKRAINSKIY FIZICHESKIY ZHURNAL in Russian Vol 36 No 11, Nov 91 pp 1713-1720

[Article by T. N. Kovalchuk, S. A. Nepiyko, I. I. Khodos, Physics Institute at the Ukrainian Academy of Sciences, Kiev]

UDC 539.216

[Abstract] Interest in studying the habitus and orientation of particles epitaxially grown by a three-dimensional mechanism on an orienting substrate is attributed to the desire to understand the formation mechanism; to this end, an Au/NaCl system is used to examine the formation conditions of multiply twinned particles, their mutual orientation and position on the substrate, and the twinning conditions during their growth leading to the development of a solid epitaxial film. Gold particles are prepared by the method of thermal sputtering in a vacuum onto a (001) cleavage of a NaCl single crystal and the habitus, mutual orientation, and position of the particles as a function of their size as well as the deposition rate, substrate temperature, annealing duration, and pressure are investigated. Two orientations of multiply twinned and single crystal particles are discovered: parallel and nonparallel. The conditions for preparing multiply twinned particles of the same kind in the same position are established. It is shown that in order to produce perfect epitaxial layers, it is important to ensure the growth conditions of not only exclusively monocrystal but also equally oriented particles. Dislocations developing during the twinning of single crystal particles disoriented by some 2-3° in the course of their growth are observed. Figures 5; references 6: 4 Russian, 2 Western.

Effect of High-Frequency Vibrations on Wavefront Orientation in Ring Resonator

927J0053A Moscow IZVESTIYA AKADEMII NAUK SSSR: MEKHANIKA TVERDOGO TELA in Russian No 3, May-Jun 91 pp 134-142

[Article by Ye. P. Kubyshkin, Yaroslavl]

UDC 624.07:534.1

[Abstract] A thin ideally circular inextensible ring (radius R) is considered which performs undamped mechanical vibrations in its plane upon excitation with a harmonically alternating voltage $V(t) = V_0\cos(\lambda_0 t)$ by a concentric outer electrode while both rotate with a constant angular velocity Ω about the axis through their common center perpendicular to their plane and at the same time both together perform small-amplitude high-frequency vibrations $p(t) = \nu \sin(\omega t)$ about some diametral axis in the plane of rotation. The ring is made of a viscoelastic $\sigma = E[\varepsilon(t) - \text{Int}_{-\infty}^{0} R(\tau)\varepsilon(t + \tau)\tau]$ material (σ - stress, ε - strain, E - modulus of elasticity, R - relaxation kernel). The behavior of such a mechanical system is described by a system of three nonlinear equations of dynamics in polar coordinates r,θ. These equations are a generalization of those for an elastic inextensible ring which takes into account viscoelasticity of the ring material and presence of external electric forces. They are obtained by application of Hamilton's variational principle and minimization of the action functional, the latter being equal to a double definite integral of the Lagrangian (density of kinetic energy minus density of potential energy) with respect to space coordinate s (length of arc from reference point to given point of ring) from s_1 to s_2 and of time t from t_1 to t_2. The resulting system of three ordinary differential equations of dynamics for this ring is rewritten in dimensionless variables and then reduced to one equation in operator form, upon introduction of the vector-function $u = \text{col}(\theta_1, r_1, \lambda)$ with the undetermined Lagrangian multiplier $\lambda(s,t)$ as third argument. The initial-value problem for this equation is analyzed and solved by the Kubyshkin method (Ye.P. Kubyshkin; DIFFERENTSIALNYYE URAVNENIYA Vol 25 No 4, 1989), which reduces it to two systems of ordinary differential equations in "slow" variables with a globally stable invariant hypersurface $r_{n1} = r_{n2}$ and in "fast" variables without limit cycles respectively. The steady-state solution to these two systems of equations and thus to that operator equation is, depending on the angular velocity of the rotating mechanical system, an either standing two-frequency wave or a precessing two-frequency wave obtained by superposition of high-frequency vibrations on the parametrically excited harmonic vibrations. The solution yields also the angle of wavefront rotation as a function of time and the angle of wavefront precession. Only two wavefront orientations are shown to be possible, a stable one at angle $\theta_n = 0$ and an unstable one at angle $\theta_n = \pi/2n$, when the ring-electrode system does not rotate ($\Omega = 0$). The author thanks V. F. Zhuravlev for very helpful discussion of the results. Figures 2; references 4.

Intensity of Superradiation

927J0054A Moscow TEORETICHESKAYA I MATEMATICHESKAYA FIZIKA in Russian Vol 88 No 1, Jul 91 pp 3-6

[Article by M. T. Turayev, Tashkent Polytechnic Institute, Beruni]

[Abstract] An exact expression for the intensity of superradiation as a function of atomic variables only is derived for the case of adiabatic atom-field interaction in open space. It is based on the superradiation Hamiltonian according to the Dicke model for two-level atoms with conservation of the total number of excitations. The equation of motion for the photon operators, the latter in the Heisenberg representation, is solved with the aid of Bogolyubov's lemma and the averages over atomic operators are obtained from the exact hierarchical equation. An equation is then derived for the time in which the correlations are homing as photon-radiator exchange occurs during spontaneous emission of radiation and attendant amplification of the initial noise field. For the case of superradiation in a resonator cavity with a finite Q-factor, the superradiation Hamiltonian must include interaction with "loss oscillators" and the equation of motion can be solved by the Weiskopf-Wigner method, which reduces it to the Heisenberg-Langevin equation. This equation accounts for the dependence of the superradiation intensity not only on spontaneous radiation emission, amplification of the initial noise field, and cooperative radiation emission, but also on dissipation processes which will accelerate formation of a superradiation emission pulse and make it asymmetric about its maximum. References 8.

Propagation and Interaction Dynamics of Electromagnetic Field Clots in Two-Level Media

927J0064A Moscow ZHURNAL EKSPERIMENTALNOY I TEORETICHESKOY FIZIKI in Russian Vol 100 No 3(9), Sep 91 pp 762-775

[Article by E. M. Belenov, A. V. Nazarkin, V. A. Ushchapovskiy, Physics Institute imeni P. N. Lebedev at the USSR Academy of Sciences]

[Abstract] Propagation of short and powerful wave packets in linear and nonlinear media and the difficulty of describing the resulting wave processes are addressed. The properties of solutions of precise Maxwell-Bloch equations (MB) are examined analytically and numerically in the cases of both absorbing and amplifying media. A study of the collision of pulses within a wide range of their initial characteristics made it possible to ascertain their parameter domains within which a quasisoliton interaction occurs. A new category of nonstationary nonlinear solutions in the form of wave packets shifting toward the blue spectral region is found in the case of an amplifying medium. These packets' energy rises not due to an increase in the number of photons in the pulse but due to an increase in each photon's energy as the pulse propagates in the medium. A similarity

between pulse propagation in a two-level medium and the electromagnetic field evolution in planar Josephson structures is discovered, making it possible to extend the findings to the electrodynamics of flaky high-T_c superconductor fields. Based on this analogy, the concept of "population inversion" is introduced and interpreted. Figures 4; references 21: 13 Russian, 8 Western.

Interference of Radiative Spatially Multimode Squeezed States and Quantum Noise-Free Control of Light Wave Fronts

927J0064B Moscow ZHURNAL EKSPERIMENTALNOY I TEORETICHESKOY FIZIKI in Russian Vol 100 No 3(9), Sep 91 pp 780-790

[Article by I. V. Sokolov, Leningrad State University]

[Abstract] The appearance of photon (shot) noise in spatially squeezed multimode light states both in the domain of time and space, i.e., in the luminous flux's transverse cross-section, is discussed and the problem of obtaining optical images without quantum noise is solved. To this end, the light wave front is controlled in a spatially multimode squeezed state with the help of an interference mixer extending in the transverse direction. Thus, the method of controlling nonclassical light fields by means of interference is applied to the three-dimensional space-time domain. The interference mixer transmittance is externally controlled in the process. Wave phase matching conditions in the squeezed light sources and in the interference mixer device are established; the characteristic quantum noise damping scales and the role of squeezed radiation diffraction as well as the possibility of reconstructing the spatial resolution of noise-free control to its limit are discussed from the space-time and spectral viewpoints. It is suggested that Faraday's rotation and birefringence be used to control the light wave front. Figures 3; references 17: 8 Russian, 9 Western.

Low-Frequency Noise and Photoinduced Light Scattering in Photorefractive Crystals

927J0064C Moscow ZHURNAL EKSPERIMENTALNOY I TEORETICHESKOY FIZIKI in Russian Vol 100 No 3(9), Sep 91 pp 1071-1076

[Article by B. I. Sturman, Automation and Electrometry Institute at the Siberian Branch of the USSR Academy of Sciences]

[Abstract] The tremendous nonlinearity of photorefractive crystals (FRK) ($LiNbO_3$ $BaTiO_3$, etc.) and the property of photoinduced light scattering (FIRS) inherent in most such crystals, making it difficult to use them for many purposes, are discussed and a new interpretation of photoinduced light scattering is suggested. The abnormally high photoinduced scattering in photorefractive crystals is attributed to the presence of the low-frequency $1/f$ noise in optical system elements and the medium, i.e., the lasing intensity noise, refractive index noise, crystal surface vibrations, etc., which causes a sharp increase in the seed scattering; the interpretation is based on the known fact that the photorefractive crystal's gain depends substantially on the detuning between the pump frequency and scattered wave frequency. Specific amplification mechanisms are considered and their behavior is predicted. It is noted that the findings can be largely applied to any medium with a high nonlinearity inertia. Figures 2; references 12: 7 Russian, 5 Western.

Theory of Suppression of Electron-Phonon Interaction in Strong Field of Coherent Light Pulse

927J0067C Moscow ZHURNAL EKSPERIMENTALNOY I TEORETICHESKOY FIZIKI in Russian Vol 100 No 8, Aug 91 pp 678-692

[Article by E. A. Manykin and M. N. Belov, Institute of Atomic Energy imeni I. V. Kurchatov]

[Abstract] Interaction of a resonance pulse of coherent optical radiation and a semiconductor during direct interband transitions is analyzed, taking into account electron-phonon scattering in the coherent field of that pulse. A theory of this interaction is constructed which will indicate how the characteristic coherence decay time depends on the intensity of the external optical field. A square light pulse of a duration τ_{pu} longer than the characteristic relaxation time τ for excess carriers is considered for which the condition $\Omega\tau > 1$ of a strong optical field is satisfied (Ω-Rabi frequency). The theory is based on the interaction Hamiltonian which $H = H_0 + H_i + H_{ph}$ representing interaction of electrons with holes, with the optical field, and with phonons. The electric field of the light wave is assumed to have an intensity with a slowly varying amplitude. From this Hamiltonian are obtained, by the method of secondary quantization and by application of the standard decoupling procedure, equations of motion of current carriers (electrons and holes) in the semiconductor. From these equations of motion are then derived equations of kinetics describing the evolution of quantum-mechanical mean electron and hole concentrations, useful for examination the evolution of both the excess carrier population (net electron concentration) and the polarization induced by the external optical field during interband transitions in the semiconductor. The coherent solution to this system of equations is shown to be the sum of a "zeroth-order" harmonic and an "oscillating" harmonic, the frequency of the latter being determined by the Rabi frequency and the deviation from resonance. An analysis of this solution for the effect of electron-phonon scattering on coherent interaction of the external optical field and the semiconductor electrons reveals that increasing the field intensity inhibits electron-phonon scattering and thus relaxation of excess carriers so that decay of the interaction coherence may be prevented. For ultrashort light pulses and correspondingly negligible relaxation of

excess carriers, moreover, the coherent solution is analogous to the coherent solution for a two-level atom in a constant external field. The difference between the two solutions is a nonuniform widening of the spectrum as determined by the dispersion relations in the energy bands in the case of a semiconductor and an ultrashort light pulse. The authors thank P. P. Vasilyev, I. S. Mukhin, and N. A. Chernyshev for assistance and helpful discussions. References 23.

Autowave Holography

927J0071D Leningrad PISMA V ZHURNAL TEKHNICHESKOY FIZIKI in Russian Vol 17 No 13, 12 Jul 91 pp 73-75

[Article by Yu. I. Balkarey and M. I. Yelinson, Institute of Radio Engineering and Electronics, USSR Academy of Sciences, Moscow]

[Abstract] The problem of using autowaves and autosolitons for holographic recording of the interference patterns of coherent linear waves is analyzed, stationary single striae being suitable for use as elements of a holographic memory. Solitary traveling pulses are not suitable for conventional interference holography, inasmuch as they annihilate each other rather than interfere with each other upon their crossing. An analysis of autowave generation in multilayer active media demonstrates, however, the feasibility of an analogous holography with autowaves. The analysis is based on the Balkarey-Yevtikhov-Yelinson model of an autowave medium (ZHURNAL TEKHNICHESKOY FIZIKI Vol 57 No 2, 1987) $dV_i/dt = 2\delta_i(V_i - V_i^3/3) - N_i + \gamma_{ij}(V_j - V_i + D_V^{ii}\Delta_{pl}^2 V_i$ and $dN_i/dt = \omega_{oi}^2(V_i - b_iN_i - a_i) + \gamma[\text{bar over } \gamma]_{ij}(N_j - N_i) + D_N^{ii}\Delta_{pl}^2 N_i$ with boundary conditions of zero derivatives of V_i and N_i, equivalent to impermeability of the medium boundaries to V and N fluxes. Each layer i,j consists of Van der Pol oscillators interacting in the diffusion mode characterized by coefficients γ_i and $\gamma[\text{bar over } \gamma]_{ij}$, ω_{oi} denotes their frequencies, $\delta_i > 0$ denotes the coefficient of negative (anomalous) amplifying friction between them, and the Laplace operator Δ_{pl} acts in the plane of a layer. The oscillators can, depending on the selection of parameters a_i and b_i, act in the self-excitation, driven, or trigger mode. Traveling pulses in different layers of the medium can, depending on the combination of γ_{ii} and $\gamma[\text{bar over } \gamma]$, weakly interact: in a triple-layer medium a single stria will form in the middle layer within the region across which oppositely traveling pulses in the outer two layers pass each other. The traveling pulses will then drift in opposite directions toward the edges of the medium and vanish at its boundaries, while the single stria will remain in its location. In the reverse process a traveling pulse in one of the outer layers will, while passing over a single stria in the middle layer, form with it two oppositely traveling pulses in the other outer layer. In a double-layer medium a traveling pulse in one layer produces a traveling pulse or a single stria in the other layer. The mechanism of such actions is extended to and demonstrated on a holographic autowave memory consisting of four layers, the outer two layers parallel to each other and in quadrature also parallel to the other inner two layers. All four layers are cut into strips so that strips in one layer will interact with corresponding orthogonal strips in the adjacent layer. This process has the basic features of plain wave holography, particularly the associative property, but phase relations between waves at different points are replaced by pulse-time relations. Figures 1; references 6.

On Theory of Self-Induced Transparence in Focused Light Beam

927J0079A Moscow PISMA V ZHURNAL EKSPERIMENTALNOY I TEORETICHESKOY FIZIKI in Russian Vol 54 No 5, Sep 91 pp 266-269

[Article by V. V. Kozlov, E. Ye. Fradkin, Scientific Research Institute of Physics at the Leningrad State University, Petrodvorets]

[Abstract] The phenomenon of self-induced transparence during a coherent interaction of ultrashort high-power Gaussian light pulses with a resonant medium is summarized and the shortcoming of the planar wave approximation is discussed. The wave equation is examined in a radially symmetric case in an approximation of slowly varying amplitudes and phases. In so doing, attention is focused on the steady-state self-sustained wave solution. As a result, a solution which is a product of the McHall-Hahn soliton by the Laguerre-Weber function is found. The solution pertains to a medium with a uniformly broadened spectral line. The solution contains a characteristic pulse frequency shift toward the red spectrum region from the absorption line center. The beam propagation velocity is found to be substantially higher than that of a planar wave whereby the velocity increases with the transverse mode number. The solution may also be extended to the case of a nonuniformly broadened absorption line. The authors are grateful to V. S. Yegorov and N. M. Reutov for constructive discussions of the consistency of these results and their experimental data. References 5: 3 Russian, 2 Western.

Dynamics of Plasma Compression by Exploding Layer in Magnetic Field

927J0067B Moscow ZHURNAL EKSPERIMENTALNOY I TEORETICHESKOY FIZIKI in Russian Vol 100 No 8, Aug 91 pp 433-439

[Article by P. Ye. Aleksandrov and V. I. Bergelson, Special Projects Department at Institute of Geophysics imeni O. J. Schmidt, USSR Academy of Sciences]

[Abstract] Plasma compression by the magnetic field of a much colder and denser liner is considered, this being an effective method of producing ultrastrong pulsed magnetic fields. Acceleration of the liner to a high velocity can be accomplished by various means, laser radiation or a particle beam among them. Not all of the thus supplied energy will be necessarily converted into kinetic energy of the liner, however, some of it being converted into internal energy instead. Cumulation of buffer plasma during this process will then be accompanied by expansion of the exploding layer so that the energy transfer from the liner to the magnetic field becomes much less efficient. The magnetic pressure and maximum plasma compression ratio η_{max} attainable under such conditions are being estimated on the basis of the following model: "inside a quiescent buffer plasma occupying a half-space there has been, at time $t = 0$, formed a hot plane plasma layer whose thickness h_0 is much smaller than its distance l_0 from the adiabatic wall or plane of symmetry and whose density ρ_0 is much higher than ρ_{00} of the buffer plasma; the initial surface density of energy in this layer is E_0 and the magnetic field parallel to the layer is initially uniform with an intensity H_0; initial gas-kinetic energy and specific internal energy of the buffer plasma are negligible." The buffer plasma and the hot plasma layer are assumed to have the same adiabatic exponent (ratio of specific heats) γ. The two controlling parameters are the dimensionless energy $\varepsilon = 8\pi E_0/(H_0^2 l_0) >> 1$ and mass $\mu = \rho_0 h_0/\rho_{00} l_0)8\pi)$ of the expanding hot plasma liner layer. Assuming a negligible increase of entropy in successively weaker reflected shock waves and compression of the buffer plasma to be an adiabatic process throughout, for estimation of the final and thus maximum compression ratio is used the relation $\eta_{max}^2 + C(\gamma)M_A^2\eta_{max}^\gamma = (\gamma + 1)\varepsilon/2$. In this expression $M_A = V_0/c_{A0} = (\varepsilon/\mu)^{1/2}$ denotes the Alfven-Mach number for the liner (V_0 - velocity of liner at the instant of collapse, c_{A0} - Alfven speed) and $C = (\gamma + 1)(3\gamma - 1)/(\gamma - 1)[(\gamma - 1)^2/\gamma(\gamma + 1)]^\gamma$ is a constant). The magnetic pressure is accordingly higher than the gas-kinetic pressure when $\eta_{max} > C(\gamma)^{1/(2-\gamma)}M_A^{2/(2-\gamma)}$ so that magnetic braking of the liner takes effect and the maximum compression ratio is $\eta_{max} \approx [(\gamma + 1)/2]^{1/2}\varepsilon^{1/2}$ when $M_A < 1$. Calculations for $\varepsilon = 100$ and $M_A \approx 0.63$ have yielded $\eta_{max} \approx 12$. The maximum plasma compression ratio is also estimated on the basis of a system of one-dimensional single-flow MHD equations which describes the process with diffusion of the magnetic field taken into account and its solution for the standard boundary conditions $u(0,t) = (\delta H/\delta x)(0,t) = 0$. This system of equations was solved numerically according to a completely conservative implicit Lagrange difference scheme and using the equation of state of an ideal gas with $\gamma = 5/3$. The electrical conductivity of all plasma has been assumed to be constant, considering that compression takes place under conditions close to those of a frozen-in magnetic flux so that the temperature dependence of the electrical conductivity is indeed negligible. The solution for $\varepsilon = 100$ and M_A has yielded $\eta_{max} \approx 15$. The authors thank I. V. Nemchinov for helpful consultations. Figures 4; references 7.

Experimental Study Concerning Effective Matching of Magnetic Blasting Generators to Radiative Plasmadynamic Discharges

927J0073C Leningrad ZHURNAL TEKHNICHESKOY FIZIKI in Russian Vol 61 No 5, May 91 pp 103-109

[Article by N. P. Bidylo, V. N. Veselov, V. A. Demidov, A. N. Demin, S. A. Kazakov, A. S. Kamrukov, N. P. Kozlov, Yu. S. Protasov, I. K. Fetisov, D. V. Chepegin, V. K. Chernyshev, and S. G. Shashkovskiy, Moscow State Technical University imeni N. E. Bauman and Scientific Research Institute of Power Apparatus Construction]

[Abstract] An experimental study of magnetic blasting generators energizing high-current plasmadynamic discharges in magnetic plasma compressors was made, the efficiency of a helical magnetic blast generator matched to a real plasma load being of concern. Two variants of such a generator were tested, each electrically loaded by plasmadynamic discharges in the compressor chamber under vacuum with an approximately 0.01 mm Hg residual pressure or containing normal air. Each generator had a 600 mm long helical winding with a 100 mm inside diameter around a heavily insulated aluminum-alloy inner tube carrying 1.5 kg of an explosive substance. The winding of the slower first variant with an initial inductance of 20 μH consisted of nine 48 mm long segments and a 120 mm long one, the winding pitch increasing from 6 mm in the first segment to 96 mm in the last one. The winding of the faster second variant with an initial inductance of 170 μH consisted of five 48 mm long segments, seven 24 mm long segments, and a 100 mm long one. Here the winding pitch increased from 2.25 mm in the first segment to 48 mm in the last one. The inner tube consisted of a 440 mm long cylinder with a 55 mm outside diameter with a 160 mm long conical extension whose diameter widened to 70 mm at the entrance to the discharge chamber of the compressor. The compressor was of the erosion type with electrodes in a coaxial-cylindrical configuration: the 20 mm in diameter cathode-rod surrounded by a 30 mm thick layer of teflon insulation inside the 80 mm in diameter anode-shell. The composition of the electric-discharge plasma was determined principally by the products of insulator erosion. An initial magnetic flux of 0.5 Wb inside the generator tube was produced by discharge of a capacitor across the winding, the capacitor having been charged to a voltage which was varied over the 5-15 kV

range. Initial current conduction in the compressor chamber under vacuum was ensured by spontaneous breakdown of the interelectrode gap. Leakage of magnetic flux from the compressor chamber during discharges through air in the initial stage of generator operation was minimized by connecting an electric fuse, four thin (0.1 mm) copper wires, across the compressor electrodes. This fuse acted as a short circuit during the initial stage of generator operation and, after a given time of about 20 μs, was ruptured by the generator current. Electrical performance parameters (current, power) were measured with Rogowski loops through voltage dividers. Evolution of discharges (plasma front velocity) was recorded with high-speed streak cameras in both slit scan and time lapse modes. Spectral and energy characteristics of radiation emission by the plasma in both visible and near-ultraviolet regions were measured with photocells and pyroelectric transducers, the latter calibrated against an EV-45 standard. The experiment has demonstrated the feasibility of electrically matching a helical magnetic blasting generator, much more effectively than a planar one, to a nonlinear active inductive load such as a high-current magnetic plasma compressor with plasmadynamic discharges. The conversion of chemical energy in a 1 kg charge of explosive substance into 75-130 kJ electric energy in the plasma reached an efficiency of 1.5-2.7 percent, the generator delivering 10-20 GW power to a 1.5-2.0 MA discharge plasma with the current gain and the power gain in the electromagnetic system, about 500 and about 100 respectively. Thermal radiation at 35,000-60,000 K high temperatures constituted about one-half of the total radiation emitted by the plasma with a maximum power of about 1 GW. The results of this study indicate the feasibility of designing such generator-compressor for an even higher than 1 percent electromagnetic-to-luminous energy conversion efficiency, which corresponds to producing a luminous flux with at least 50 mJ energy per 1 kg of explosive substance. Figures 4; references 7.

Short-Wave Ion-Cyclotron Soliton

927J0075B Moscow FIZIKA PLAZMY in Russian Vol 17 No 8, Aug 91 pp 976-979

[Article by T. A. Davydova, V. M. Lashkin, Nuclear Research Institute at the Ukrainian Academy of Sciences]

UDC 533.951.8

[Abstract] The radio frequency (VCh) diamagnetism effect which is the principal nonlinear phenomenon which determines the behavior of substantially nonlinear (extending beyond the applicability of the weak turbulence theory approximation) cyclotron waves is discussed. A soliton solution is derived in the case of a quasi-transverse distribution of the short-wave potential ion-cyclotron wave which is often referred to as Bernstein's mode. These solitons' characteristics dimension is smaller than Larmor's ion radius, they are localized across the external magnetic field, and their velocity is smaller than the ions' thermal velocity. Such solitons may form as a result of the development of cyclotron instabilities in the auroral area of the earth's magnetosphere or during the RF plasma heating at a sufficiently high injected power level within the ion-cyclotron frequency band. It is assumed that the wave frequency is close to a certain harmonic of the ion-cyclotron frequency. The study revealed the existence of short-wave solitons forming on the potential ion-cyclotron oscillation branch as a result of the nonlinear RF diamagnetism effect. In addition to the small-scale coherent ion-cyclotron wave structures, electric and magnetic field "jumps" in a lower-frequency region are discovered. It is speculated that the origin of these phenomena is directly related to the aforementioned soliton formation. References 10: 6 Russian, 4 Western.

Energy Processes in Macroscopic Fractal Structures

927J0083A Moscow USPEKHI FIZICHESKIKH NAUK in Russian Vol 161 No 6, Jun 91 pp 171-200

[Article by B. M. Smirnov, High Temperatures Institute at the USSR Academy of Sciences]

UDC 533.98

[Abstract] Macroscopic fractal structures—aerogels forming from small particles in solutions and fractal filaments forming from a nonequilibrium low-temperature plasma in an external magnetic field—and small elements of such structures, i.e., fractal clusters or aggregations, are examined. The properties of such entities, as highly rarefied structures, consisting of small particles and the processes occurring inside these structures, which are similar to processes in gases but display their own specific features, are analyzed. Attention is focused on the macroscopic fractal structures' large specific internal surface and the resulting explosive behavior whereby the released energy develops a heat wave which propagates and transforms the internal energy, thus destroying the structure. In addition to thermal processes inside macroscopic fractal structures, the conditions of thermal explosion of the structure and the parameters of the resulting heat wave are investigated. An analysis shows that fractal structures are characterized in that such processes may occur in them only in relatively high temperatures; moreover, such a system may serve as an efficient source of light. This specific feature may be used for using such structures in special devices. Figures 10; tables 7; references 112: 21 Russian, 91 Western.

Transfer of Gases From Ambient Medium to Y-Ba-Cu-O Superconducting Ceramic and Medium and Fractal Character of Ceramic Based on Low-Angle Neutron Scattering Data

927J0056F Moscow ZHURNAL EKSPERIMENTALNOY I TEORETICHESKOY FIZIKI in Russian Vol 100 No 1(7), Jul 91 pp 257-273

[Article by A. I. Okorokov, V. V. Runov, A. D. Tretyakov, S. V. Maleyev, and B. P. Toperverg, Leningrad Institute of Nuclear Physics imeni B. P. Konstantinov, USSR Academy of Sciences]

[Abstract] Interaction of $YBa_2Cu_3O_{7-d}$ superconducting ceramic and gases, oxygen and nitrogen, was studied by the low-angle neutron scattering method. Measurements were made at temperatures covering the 4.2-300 K range with a neutron beam having a $\lambda = 1$ nm mean wavelength ($\Delta\lambda/\lambda = 0.3$) and with the neutron momentum q transferred in scattering ranging from 0 to 0.26/nm ($\Delta q = 0.03$/nm). Measurements at low temperatures were made in a helium cryostat. The angular distribution of scattering intensity at room temperature was measured without a cryostat. The external magnetic field was always oriented parallel to the axis of the neutron beam and its intensity never exceeded the 0.7 Oe. Two groups of ceramic $YBa_2Cu_3O_{7-d}$ specimens were tested: 1) 3 mm thick and 7 mm thick 10x30 mm^2 large bars of material whose density was 3.5 gm/cm^3, prepared at the Moscow Institute of Steel and Alloys; 2) 1.5 mm thick 8x32 mm^3 large bars of material whose density was 5.15 gm/cm^3, prepared at the Institute of Solid-State Physics in Chernogolovka. The superconducting transition temperatures were 93 K, 90 K, 84 K for the friable material and 93 K, 90 K, 85 K for the dense material at 0.95, 0.05, 0.005 levels of relative to the normal-state electrical resistance respectively. Specimens were variously annealed prior to measurements: a) in a gaseous helium atmosphere, b) in a gaseous oxygen atmosphere under various pressures (4 atm and 10 atm), c) in a gaseous nitrogen atmosphere. Specimens of the friable material had been prior to these treatments dried at 50-70°C for several hours, then fast cooled to 4.2 K within less than 30 minutes in a shaft cryostat with gaseous helium and held there for about 3 h. The temperature dependence of their electrical resistance did not reveal any anomalies even under rising oxygen pressure, this ceramic with a porous "open" structure evidently adsorbing oxygen. The data confirm, furthermore, that the critical superconducting transition temperature for this ceramic does not depend on the boiling point of oxygen. For measurement of momentum and temperature dependent neutron scattering intensity I(q,T), bars of the dense material were cut into 0.67 +/- 0.01 thick and 1 +/- 0.02 mm thick 8x15 mm^2 large slices. The slices were then combined into 0.67 mm, 1.66 mm, 2.33 mm, 3.32 mm, and 3.9 mm thick stacks, for measurement of their neutron absorption by the transmission method with a neutron detector behind the stack and for measurement of their integral neutron scattering with a set of counters including one at the center before the stack. Both coefficients were found to decrease almost linearly with increasing stack thickness, the integral scattering coefficient decreasing much faster. An analysis of the results, aided with theoretical calculations on the basis of appropriate scattering models, reveals that 100 nm wide pores and all wider ones make up most of the void volume in this high-T_c superconductor ceramic. Inasmuch as the surface of this ceramic is highly erose, it can be treated as a fractal. The excellent opening of pores at the surface ensures access of the ambient gas to all grains inside and its adsorption by the latter, oxygen much more easily permeating the ceramic than nitrogen so that the pores will be occupied by oxygen mainly when the ceramic is exposed to air. The authors thank B. Mandelbrot for helpful discussion of the results, Ye. G. Ponyatovskiy for supporting the study, N. M. Kotov, A. S. Nigmatullin, Ya. M Mukovskiy, V. K. Fedotov, R. K. Nikolayev, and N. S. Sidorov for preparing and testing the specimens, D. N. Aristov for numerical computations, L. A. Akselrod, G. P. Gordeyev, V. P. Grigoryev, V. N. Zabenkin, I. M. Lazebnik, V. T. Lebedev, V. N. Slyusar, R. Z. Yaruda, I. N. Ivanova, E. B. Rodzevich, N. M. Kusova, and G. V. Stepanova for assistance in the study and its formatting. Figures 8; tables 1; references 20.

Vortex Rings and Dissipation in Type-2 Superconductors

927J0056G Moscow ZHURNAL EKSPERIMENTALNOY I TEORETICHESKOY FIZIKI in Russian Vol 100 No 1(7), Jul 91 pp 301-306

[Article by Ye. B. Kolomeyskiy, Institute of Crystallography imeni A. V. Shubnikov, USSR Academy of Sciences]

[Abstract] Erosion of superconductivity by an external current of up to critical density j_c is analyzed in accordance with the Ginzburg-Landau theory and the essential role of energy dissipation in this process is demonstrated on type-2 superconductors. To prove that dissipationless current flow at zero temperature is not possible even though the linear electrical resistance of the superconductor may be zero, an infinitely long straight Abrikosov vortex is considered with the axis perpendicular to the direction of current flow so that the maximum force will act on it and an also favorably oriented closed vortex with a radius r much larger than the coherence length ξ will form. The energy dissipation mechanism is shown to involve periodic formation of such rings and their expansion up to and including their merger. The critical ring radius r_c, at which the energy of a vortex ring is maximum, is then inversely proportional to the current density and so is that maximum energy. At temperature $T = 0$ in a magnetic field superconductivity vanishes at a current density at which closed vortex rings with radii $r \approx \xi$ begin to appear in a process without a threshold. At temperatures $T > 0$ in a magnetic field, assuming magnetic-field penetration depth λ much larger than the coherence length ξ (Ginzburg-Landau parameter $k = \lambda/\xi > 1$) and a current density such that

the critical ring radius r_c is much larger than the magnetic-field penetration depth λ, this current density will have to be $j << j_c(\log k)/k$. In this case the dependence of the mean electric-field intensity E and correspondingly of the electrical resistivity ratio ρ/ρ_n (ρ_n - electrical resistivity in normal state) on the current density j in a layer much thicker than λ is established on the basis of the Josephson relation for the average rate of change of the difference between the order parameter phases on both sides of that layer, this average rate of change being proportional to the average voltage across the layer. In this case, the rate of energy (heat) dissipation Ej/cm^3 is proportional to $j^{7/3}\exp(-e\varepsilon^2/3hjT)$ (e - electron charge, ε - linear energy density dependent on ring radius r, h - Planck's constant). Such an E(j) dependence holds true only up to the current density at which the critical ring radius r becomes equal to the magnetic field penetration depth λ, in this limiting case the $\rho(j)/_v$ ratio being described by a simpler expression and ρ_n being estimated on the basis of the Drude-Lorentz equation. The pattern is analogous at current densities within the $j_c(\log k/k) \leq j \leq j_c$ range, but then the critical ring radius lies within the $\lambda \leq r_c << \xi$ range. In this case the rate of energy (heat) dissipation is proportional to $\exp[-\text{const.}\log^2(j_c/j)/jT]$. When the current density approaches the critical one so that $j_c - j << j_c$, then the rate of energy (heat) dissipation becomes proportional to $\exp[-\text{const.}(j_c - j)/Tj_c]$. The authors thank A. P. Levanyuk for helpful discussions. References 8.

Flux-Line Liquid Pinning in High-T_c Superconductors

927J0064E Moscow ZHURNAL EKSPERIMENTALNOY I TEORETICHESKOY FIZIKI in Russian Vol 100 No 3(9), Sep 91 pp 1104-1118

[Article by V. M. Vinokur, V. B. Geshkenbeyn, A. I. Larkin, M. V. Feygelman, Theoretical Physics Institute imeni L. D. Landau at the USSR Academy of Sciences]

[Abstract] The property of high-T_c superconductors (VTSP) whereby the resistive transition broadens considerably with an increase in the external magnetic field is discussed and attributed to a transition from the flux-line liquid state where there is no pinning, eddies are in viscous flux flow, and the volt-ampere characteristic (VAKh) is linear, to a state of pinned flux-line glass with a substantially nonlinear volt-ampere characteristic. It is shown that there are two temperature domains in the flux-line liquid with a different dependence of resistance on temperature. Pinning is insignificant at high temperatures and resistance changes exponentially with temperature while at low temperatures, resistance is proportionate to the time of plastic deformation in the flux-line liquid and depends on temperature according to the activation law. The preexponential factor in this law is determined by the pinning force. Thus, the concept of collective pinning of a very viscous flux-line liquid on weak defects explains the temperature behavior of the high-T_c superconductor's linear dependence of resistance on temperature in a strong magnetic field which is characterized by an abrupt transition from a flux flow condition to the thermally activated flux flow condition (TAFF) with an activational decrease in $\rho(T)$ with temperature. The authors are grateful to S. Doniach for pointing their attention to his articles. References 34: 2 Russian, 32 Western.

Flux Line Structure Dynamics in $Bi_2Sr_2CaCu_2O_y$ Single Crystals

927J0065B Moscow PISMA V ZHURNAL EKSPERIMENTALNOY I TEORETICHESKOY FIZIKI in Russian Vol 54 No 1, Jul 91 pp 25-31

[Article by V. N. Zavaritskiy, N. V. Zavarutskiy, Physical Problems Institute imeni P. L. Kapitsa at the USSR Academy of Sciences and General Physics Institute at the USSR Academy of Sciences, Moscow]

[Abstract] The flux line structure in high-T_c superconductors (VTSP) and its relationship to long-term relaxation processes, critical current, thermally activated sample resistance in the neighborhood of the critical temperature, and the relative height of the potential barrier for the flux creep are discussed and the dynamics of the flux line structure in $Bi_2Sr_2CaCu_2O_8$ (Bi-2212) single crystals in $H\|$ are investigated within a broad temperature range of 4.2 to $(T_c - T) < 1$K. Remanent magnetization induced in Bi-2212 normal-stoichiometry crystals cooled beforehand in a zero field below T_c (ZFC) and in a sample cooled in an external field (FC) is measured after the external field is lifted. A qualitative change in the flux line structure dynamics of Bi-2212 single crystals at a T_j close to (17 +/- 1) K temperature is established; this is manifested by an almost tenfold abrupt change in the normalized logarithmic flux rate creep, a sharp change in the remanent magnetization's dependence on temperature, and a change in the dependence of the potential barrier height on the superconducting current density. It is also established in the experiment that $U_o \rightarrow \infty$ given $T \quad T_c$. The results indicate that T_j temperature plays a special role in the flux line structure dynamics in Bi-2212 crystals: It separates areas characterized by different types of the critical current behavior in the temperature domain manifested by differences in the vortex pinning and/or vortex structure. The authors are grateful to A. I. Larkin and M. V. Feygelman for numerous useful discussions and A. A. Yurgens for providing an automated SQUID magnetometer and making valuable remarks. Figures 4; references 22: 1 Russian, 21 Western.

Magnetoresistance and Metamagnetic Transition in $La_2CuO_{4+\delta}$ With Low Neel Temperature

927J0065C Moscow PISMA V ZHURNAL EKSPERIMENTALNOY I TEORETICHESKOY FIZIKI in Russian Vol 54 No 1, Jul 91 pp 32-35

[Article by A. A. Zakharov, A. A. Teplov, Ye. P. Krasnoperov, M. B. Tsetlin, A. K. Tsygankov, S. N. Barilo, P. V. Gritskov, Atomic Energy Institute imeni I. V. Kurchatov, Moscow]

[Abstract] Magnetoresistance of $La_2CuO_{4+\delta}$ single crystals with a Neel temperature below 170K is investigated in the $H \| c, j \| c$ geometry using a tetragonal designation of axes; this makes it possible to examine the metamagnetic transition from an antiferromagnetic phase state (AF) to weakly ferromagnetic phase state (SF). In order to ascertain the relationship between magnetic and transport phenomena, the dependence of magnetic moment on magnetic field is investigated in such samples with the help of a magnetometer within a 4.2-200K temperature range. Parallelepiped-shaped single crystals are examined. An abnormal increase in the magnetoresistance and magnetization hysteresis during a metamagnetic transition is discovered in $La_2CuO_{4+\delta}$ single crystals with a Neel temperature of about 165K when they are cooled to below 20K. A decrease in the magnetic resistance jump is also established in these samples. Both phenomena are attributed to a return transition from the antiferromagnetic to the weakly ferromagnetic phase. The authors are grateful to A. N. Bazhan, A. S. Ioselevich, L. B. Dubovskiy, and S. N. Burmistrov for discussing the findings and to A. N. Bazhan for examining the magnetic properties of $La_2CuO_{4+\delta}$ samples. Figures 2; references 10: 3 Russian, 7 Western.

Two Pinning Mechanism in $Bi_{2+x}Sr_{2+y}Ca_{1+x}Cu_2O_t$ Phase Single Crystals

927J0066C Moscow PISMA V ZHURNAL EKSPERIMENTALNOY I TEORETICHESKOY FIZIKI in Russian Vol 53 No 9, May 91 pp 466-469

[Article by A. A. Zhukov, V. V. Moshchalkov, V. A. Rybachuk, V. A. Murashov, I. N. Goncharov, Moscow State University imeni M. V. Lomonosov, Radio Engineering, Electronics, and Automation Institute, Moscow, and Joint Institute for Nuclear Research, Dubna]

[Abstract] The critical current density behavior within a broad range of temperatures, the effect of various types of pinning centers on the critical current density, and the phenomenon of magnetic flux creep are discussed. The dependence of critical current density in temperature in the basal plane of $Bi_{2+x}Sr_{2+y}Ca_{1+x}Cu_2O_t$ phase single crystals and the effect of their irradiation with Ar ions at a 15 MeV/nucleus energy is investigated. The value of critical current density is determined by the magnetic moment hysteresis measured after boosting the field to a level greater than the field of sample center penetration by the eddies and decreasing the external field to zero. The temperature dependence of critical current density is characterized by two temperature intervals. Remanent magnetization relaxation corresponding to the cooling of the sample in the field and decreasing it after reaching the requisite temperature is also investigated. The crystals display an abrupt increase in the critical current density (by several orders of magnitude) after irradiation with Ar^+ ions. An analysis of the magnetic flux creep as well as the dependence of critical current density on temperature and magnetic field indicates an intrinsic low-temperature pining mechanism and a high-temperature pining mechanism related to defects, e.g., dislocations, superstructure block boundaries, and other single crystal imperfections. Relaxation processes have a significant effect on the critical current density which is especially strong in the 8-24K temperature range. The effort is supported by the Scientific Council on high-T_c superconductivity and is carried out at the BAZIS VNK in the framework of projects Nos. 90061 and 421 of the state program of high-T_c superconductivity. Figures 3; references 13: 2 Russian, 11 Western.

Theory of Nonlinear Electrical Conductivity of Superconductor Point Junctions Containing Magnetic Impurities

927J0068C Kharkov FIZIKA NIZKIKH TEMPERATUR in Russian Vol 17 No 8, Aug 91 pp 994-998

[Article by S. I. Beloborodko and A. N. Omelyanchuk, Institute of Low-Temperature Engineering Physics, UkSSR Academy of Sciences, Kharkov]

UDC 538.945

[Abstract] The effect of magnetic impurities in an S-c-N tunnel junction is analyzed, considering that the current-voltage characteristic of a pure such junction under a voltage $eV >> \Delta_0$ is $I(V) = V/R + I_{ex}$ and the excess current I_{ex} is equal to $C\Delta_0/R$ (C - numerical coefficient: C = 4/3 for pure junction and C = 0.73 for dirty junction). The analysis is based on the two Eliashberg integral equations for superconductors with magnetic impurities, one for $(1 - z(\varepsilon))\varepsilon$ and one for $z(\varepsilon)\Delta(\varepsilon)$ They are solved in the B-C-S approximation so that in the absence of magnetic impurities the energy-dependent order parameter $\Delta(\varepsilon)$ would become equal to the superconductor's energy gap Δ_0. As to electron-phonon interaction, its delaying effect is disregarded but the resulting decay of electronic states and breaking of electron pairs is accounted for by retention of the imaginary part of the kernel $K(\varepsilon',\varepsilon)$ in the equation for $(1 - z(\varepsilon))\varepsilon$. The temperature dependence of the excess current in a pure superconductor and in a gapless one is then calculated, over the $0 \leq T \leq T_c$ temperature range, with the aid of the Abrikosov-Gorkov relation describing the temperature dependence of the order parameter $\Delta^2(T)$. The dependence of the differential electrical conductance dI/dV at zero temperature on the junction voltage is calculated and then plotted in the form of dimensionless R(dI/dV) vs. eV/Δ_0 curves (R - electrical resistance) for various values of the Γ/Δ ratio (Γ - pair breaking parameter). As the value of Γ parameter is increased from 0 to 1.1 so as to characterize a correspondingly increasing concentration of magnetic impurities from zero level up, the temperature dependence of the excess current in the superconductor degenerates from a square-root dependence to a linear one and the singularity of nonlinear electrical conductivity of the S-c-N junction becomes blurred while it shifts toward a lower energy. The results of this theoretical analysis and calculations are validated by experimental data on high-T_c superconductors with

magnetic impurities. The authors thank I. O. Kulik for valuable comments, also A. I. Akimenko and A. L. Solovyev for discussion of experimental data. Figures 2; references 8.

Spin-Spin Relaxation of $^{63}Cu(2)$ Nuclei and Localized $Cu^{2+}(2)$ Centers in $YBa_2Cu_3O_{7-d}$ Ceramic

927J0069C Moscow PISMA V ZHURNAL EKSPERIMENTALNOY I TEORETICHESKOY FIZIKI in Russian Vol 54 No 3, 10 Aug 91 pp 154-159

[Article by O. A. Anikeyenok, M. V. Yeremin, R. Sh. Zhdanov, V. V. Naletov, M. P. Rodionova, and M. A. Teplov, Kazan State University]

[Abstract] An experimental study of nuclear quadrupole resonance (NQR) in $YBa_2Cu_3O_{6.95}$ and $YbBa_2Cu_3O_{6.9}$(Yb) high-T_c superconductor ceramics was made concerning spin-spin relaxation of $^{63}Cu(1)$ and $^{63}Cu(2)$ nuclei. The object of this study was the field dependence of the relaxation speed $1/T_2$ (T_2 - relaxation time) in an external magnetic field at 4.2 K temperature, its temperature dependence having already been studied and the NQR line found to be a Gaussian one with the ratio of fourth moment to second moment squared $M_4/M_2^2 \approx 3$ at temperatures $T > T_c$ and to be a Lorentz line with this ratio ranging from six to 10 at temperatures $T < T_c$ (approximately 10 at 4.2 K as well as at 35 K). Specimens of Y ceramic (T_c = 93 K, $\nu_{Cu(1)}$ = 22.0 MHz, $\nu_{Cu(2)}$ = 31.5 MHz) and Yb ceramic (T_c = 83 K, $\nu_{Cu(1)}$ = 22.05 MHz, $\nu_{Cu(2)}$ = 30.9 MHz) were prepared by the standard method, their single 1-2-3 phase composition being monitored by X-ray phase analysis and their critical superconducting transition temperature being determined from the temperature dependence of their magnetic susceptibility. The intensity of the external magnetic field was varied over the 0-200 Oe range. The full width of the NQR line at half-amplitude level $\Delta\nu_{0.5}$ was: 400 kHz for Cu(1) and 600 kHz for Cu(2) in Y-Ba-Cu-O, 1.3 kHz for Cu(1) and 1.6 kHz for Cu(2) in Yb-Ba-Cu-O. The spin-spin relaxation time was measured with a coherent pulsed laboratory spectrometer. Relaxation of Cu(1) nuclei in both ceramics was found to become slower upon application of a magnetic field, replacement of the diamagnetic Y^{3+} ions with the paramagnetic Yb^{3+} ions not resulting in any noticeable increase of the in relaxation speed. Relaxation of Cu(2) nuclei in Y-Ba-Cu-O was found to become faster upon application of a magnetic field, its speed increasing to a maximum within the 40-50 Oe range after passing through small but discernible peaks at about 5 Oe and about 15 Oe, then to become slower with further increase of the field intensity. Relaxation of Cu(2) nuclei was found to proceed much faster in Yb-Ba-Cu-O than in Y-Ba-Cu-O at zero field intensity, owing to their strong spin-spin interaction with nearby magnetic Yb^{3+} ions, and then to increase upon application of a magnetic field to a maximum at 40 Oe after passing through a higher than in Y-Ba-Cu-O peak at about 5 Oe. These data indicate that Cu(2) nuclei are strongly coupled to some paramagnetic centers by spin-spin interaction and that Cu(1) nuclei are not coupled to such centers, these centers thus evidently being localized in the CuO_2 planes. These centers are shown to be Cu^{2+} ions located in the immediate vicinity of resonating Cu(2) nuclei, which belong to the superconducting phase. This hypothesis is supported by a theoretical and numerical analysis of energy levels in the Cu^{2+} ion in a weak magnetic field. Calculations are based on the interaction Hamiltonian of a $^{63}Cu^{2+}$ ion in a magnetic field oriented at an arbitrary angle φ to the Y-Ba-Cu-O or Yb-Ba-Cu-O crystal axis and probability of electronic transitions at the $\nu_{Cu(2)}$ frequency in the system of electronic and nuclear energy levels. The state of Cu atoms whose nuclei participate in both nuclear-quadrupole and nuclear-magnetic resonances in these high-T_c superconductors is not yet definitively known, but the experimental data meantime confirm that their state in CuO_2 planes correspond to ordinary localized Cu^{2+} centers. The acceleration of spin-spin relaxation of Cu(2) nuclei could, moreover, be caused by spin-lattice relaxation of these localized Cu^{2+} centers. The authors thank A. F. Andreyev for discussion. Figures 3; references 18.

Superconductivity Stimulation in Multilayer Metal-Oxide Superconductors

927J0072B Leningrad FIZIKA TVERDOGO TELA in Russian Vol 33 No 2, Feb 91 pp 504-507

[Article by V. A. Cherenkov, USSR State Committee for Standards and V. Ye. Grishin, All-Union Scientific Research Institute of Metrological Service, Moscow]

UDC 530.1+539.2

[Abstract] Superconductivity stimulation in multilayer Nb-NbO_x-Nb structures is considered, such a structure with 1-2 nm thick oxide layers between 10-40 nm thick Nb layers being a quasi-two-dimensional one inasmuch as a transverse current flows in the layers after superconducting transition has taken place (T_c about 4.9 K) and the current between layers does not wipe out superconductivity. While the dependence of the superconducting transition temperature for multilayer metal superconductors on the number of layers and on their thickness has already been determined by B. Y. Shapiro and L. V. Yefimova (PHYSICA STATUS SOLIDI Vol 144B, 1987) using the model of nonuniform electron-electron interaction in metal superconductors, the superconducting transition temperature for a multilayer metal-oxide-metal structure with weak Josephson interaction between layers is calculated by four methods: 1) on the basis of the tunneling Hamiltonian and the applicable system of linearized sine-Gordon equations, the Schroedinger equation being written for a sandwich structure in discrete states; 2) on the basis of the anisotropic two-dimensional Ising model of a Josephson XY-lattice with weak interaction; 3) by introduction of an external pinning potential into the multilayer structure; 4) on the

basis of the XY-model of a multilayer structure with frustration. The authors thank Ye. A. Shapovalov for interest. References 13.

Flux Creep Effects in Microwave $YBa_2Cu_3O_x$ Single Crystal Absorption

927J0076B Moscow PISMA V ZHURNAL EKSPERIMENTALNOY I TEORETICHESKOY FIZIKI in Russian Vol 54 No 6, Sep 91 pp 342-345

[Article by Ye. F. Kukovitskiy, S. G. Lvov, Yu. I. Talanov, G. B. Teytelbaum, R. I. Khasanov, Kazan Engineering Physics Institute at the USSR Academy of Sciences]

[Abstract] The behavior of the flux-line lattice in high-T_c superconductors is discussed and the need to use new methods, such as studies of microwave absorption of superconducting single crystals, is identified. To this end, $YBa_2Cu_3O_x$ single crystals were examined in order to establish the manifestations of magnetic flux kinetics in their microwave absorption and use the resulting data to determine a number of important parameters. The study is carried out in an electron paramagnetic resonance spectrometer (BER-418s manufactured by the Bruker company) at a 9.4 GHz frequency within a 1.6-40K range. Single crystals with different critical temperatures and different twinning degrees are examined. As a result, an abnormal behavior of microwave absorption is discovered: It drops sharply with a decrease in magnetic field and rises with its increase; the phenomenon is attributed to transitions between the states of the lattice in the presence of the trapped magnetic flux. A shift of the absorbed power derivative extrema in the field is observed and described as a flux creep. The disappearance of this phenomenon at temperatures above 35K is probably due to a significant interaction among flux lines and a transition to collective pinning which is accompanied by an exponential decrease in the critical current density and fast magnetic flux relaxation. The authors are grateful to L. Ya. Vinnikov for useful discussions. The effort is supported by the Scientific Council on high-T_c superconductivity and is carried out in the framework of project No. 344. Figures 3; references: 8 Western.

Exchange Theory of Electron Pairing in Solids

927J0080A Moscow DOKLADY AKADEMII NAUK SSSR in Russian Vol 319 No 1, Jul 91 pp 161-164

[Article by A. V. Kulakov, Ye. V. Orlenko, A. A. Rumyantsev, Leningrad Polytechnic Institute imeni I. I. Kalinin]

UDC 537.312

[Abstract] Various mechanisms of long- and close-range electron pair formation in high-T_c superconductors (VTSP), the manifestations of spin correlations in superconductors, and the development of second-kind phase transitions in them are discussed; it is shown that these manifestations and phase transitions are closely related due to the universality of the quantum exchange and superexchange forces involved in these processes. An attempt is made to analyze the energy contributions determined by the exchange whose parameters are phenomenological in origin by directly balancing Bloch's wave vectors for the system of electrons. To this end, the effect of annealing on the state of high-T_c superconductor bismuth-strontium ceramics is considered since annealing compresses the crystal's lattice cell in the direction of its principal axis while simultaneously increasing the amount of oxygen and, consequently, the number of electrons participating in the exchange. The mechanism under study explains the pairing of particles at a distance of more than 10^{-5} cm; for ceramic materials, the ratio of the energy gap to T_c transition temperature expressed in units of energy is on the order of unity, which is consistent with experimental data. Thus, the fluctuation hypothesis of the superconducting state explains rather freely the characteristic features of the phenomena observed during annealing. References 5.

Low-Temperature Scanning Electron Microscopy of YBaCuO Superconductor Film Compositions

927J0081B Moscow IZVESTIYA AKADEMII NAUK SSSR: SERIYA FIZICHESKAYA in Russian Vol 55 No 8, Aug 91 pp 1543-1546

[Article by L. S. Kokhanchik, A. V. Nikulov, V. Zh. Rozenflants, A. V. Chernykh, Microelectronics and Especially Pure Materials Technology Problems Institute at the USSR Academy of Sciences]

UDC 537.533.8:537.312.62

[Abstract] The accessibility and information content value of scanning electron microscopy methods for examining high-T_c superconductor (VTSP) compounds is discussed and a study of the temperature-induced changes in the $Y_1Ba_2Cu_3O_{7-x}$ films' image contrast in the secondary electron (VE) scanning condition is reported. The dynamics of sample darkening at T_c are examined. It is shown that the image darkening dynamics in areas smaller than 10 μm are not related to the secondary electron trajectory deflection due to Meissner's effect. An increased sensitivity of films with a semiconductor behavior to electron irradiation at low temperatures manifested by an abnormal secondary electron emission is noted. It is speculated that local glow regions detected in such films under electron irradiation are due to the presence of a larger number of superconductor-semiconductor contacts than in samples with a metallic behavior. A JSM-35C microscope is used in the experiment. Figures 3; references 11: 6 Russian, 5 Western.

Study of Lower Ionosphere With Aid of Artificial Periodic Inhomogeneities

927J0057A Moscow GEOMAGNETIZM I AERONOMIYA in Russian Vol 31 No 4, Aug-Sep 91 pp 743-746

[Article by L. N. Rubtsov, A. V. Blokhin, V. Ya. Kovalev, S. F. Marchenko, V. V. Belikovich, Ye. A. Benediktov, N. P. Goncharov, A. I. Yezhov, and A. V. Tolmacheva, Gorkiy Scientific Research Institute of Radiophysics]

UDC 550.388.2

[Abstract] The lower ionosphere above the Dushanbe region was probed during the 1987-89 period, the method of resonance scattering by artificial periodic inhomogeneities being applied with the use of a special apparatus built in 1975. The apparatus consists of a 100 kW transmitter with a "Tissar" heater and a receiver of scattered signals with a multichannel amplitude recording instrument. The directional transmitter antenna has a directive gain ranging from 60 to 90. The receiver antenna is a cophasal array of six dipoles for each of the two orthogonal linear polarizations and can extract the sought circularly polarized signals coming from six fixed altitudes within both D and E layers. Artificial periodic inhomogeneities were produced by local heating of the electron gas in the loop of a standing radio wave. Both the plasma relaxation time $\tau = 1/(\beta + \gamma)$ (β - temperature-dependent coefficient of electron capture by oxygen molecule, γ - coefficient of electron separation from oxygen molecule) at lower altitudes (55-75 km) and the plasma diffusion-redistribution time $\tau = 1/(4.4k^2D_a)$ (κ - wave number, D_α - coefficient of ambipolar diffusion) at higher altitudes (90-135 km) were measured with 3860-4263 kHz radio waves in 1988 from late September to early October 1988 and in 1989 from late January to early April, mostly during evening hours. Analysis of the data reveals a seasonal variation of each plasma relaxation time. Their geographical (latitudinal) variation was evaluated by comparing the Dushanbe (38.5° N) readings with Gorkiy (56.1° N) readings and found to be in Dushanbe only 1.5 times wider in winter and 1.8 times wider in spring. The relaxation time was calculated according to two diffusion models: 1) V. V. Belikovich, Benediktov, S. A. Dmitriyev, et al.; IZVESTIYA VYSSHIKH UCHEBNYKH ZAVEDENIY: RADIOFIZIKA, Vol 24, 1981 p 905; 2) M. N. Fatkullin, T. I. Zelenova, V. K. Kozlov, et al.; "Empirical Models of Middle-Latitude Ionosphere", Izd. Nauka, 1981). Within the 80-95 km range of altitudes were repeatedly recorded waves of relaxation time variations with 5-15 min long periods, apparently caused by propagation of acousto-gravitational waves. Figures 3; references 4.

Amplitude and Phase Modulation of Vibration Speckle-Interferometer Signal

927J0071A Leningrad PISMA V ZHURNAL TEKHNICHESKOY FIZIKI in Russian Vol 17 No 13, 12 Jul 91 pp 11-15

[Article by V. P. Ryabukho and S. S. Ulyanov]

[Abstract] Measurement of the vibration parameters of rough surfaces with a laser speckle-interferometer using a speckle-modulated reference wave is considered, its output signal appearing in the photodetector aperture having a Rayleigh amplitude distribution with both mean and most probable amplitudes increasing as the number of speckles increases under conditions of large vibration amplitudes ($A > \lambda/4$, λ - wavelength) or a unilateral Gaussian amplitude distribution with zero mean amplitude under conditions of small vibration amplitudes ($A < \lambda/4$). In the latter case the mean signal amplitude is proportional, not directly to the receiver aperture diameter, but to its product by the transverse dimension of speckles in the plane of that aperture. Parasitic amplitude and phase modulation of the speckle-modulated reference wave may take place when the amplitude A of surface vibrations is sufficiently large and the number N of speckles appearing in the receiver aperture is very large, such a parasitic modulation having been in experiments with N varying from 100 to 900. This modulation is shown to result from a transverse shift of the object speckle field caused by local tilt of the vibrating surface under the laser beam relative to the reference speckle field. That the effect of a thus synthesized receiver aperture on the modulation of the interferometer output signal is determined mainly by the phase relation between object and reference speckle fields is demonstrated on a Michelson vibration speckle-interferometer, on the basis of the theoretical space-time distribution of light intensity in the interferometer exit plane and by a comparison of the theoretical distribution density function of the interferometer output signal amplitude during small-amplitude surface vibrations with the histogram of that output signal amplitude. Oscillograms of interferometer output signals reveal that inserting a small opaque blocking shield into the receiver aperture and moving it across that aperture will effectively suppress up to 100 percent parasitic amplitude modulation by some dominant speckle cluster. The authors thank A. V. Ampilogov for helpful discussion. Figures 2; references 2.

Producing Ultrawide-Band Radio Power Pulses With Resonant Shapers

927J0071B Leningrad PISMA V ZHURNAL TEKHNICHESKOY FIZIKI in Russian Vol 17 No 13, 12 Jul 91 pp 37-40

[Article by S. A. Novikov, S. V. Razin, P. Yu. Chumerin, and Yu. G. Yushkov]

[Abstract] The feasibility of producing ultrawide-band pulses of 100 MW and higher power within the 0.1-1.5 m

waveband was demonstrated in experiments with pulse shapers and with a gas-discharge switch operating in the self-breakdown mode under atmospheric pressure as a short-circuiting capacitor. Pulse shapers 1 and 2 were each a coaxial-T, pulse shaper 3 was a twin-T. They operated at their respective resonance frequencies: f_1 = 150 MHz, f_2 = 900 MHz, f_3 = 2.82 GHz. The minimum duration of UHF pulses at the output of such a shaper is determined by twice the time of wave passage through a tee arm and can be made equal to one oscillation period at the resonance frequency. In the experiment with one pulse shaper a high-frequency pulse generator applied to it, through a decoupling ferrite diode and a phase shifter, 10kW f_1-pulses of 4 μs duration and 1 kW f_2-pulses of 5 μs duration respectively. A special coaxial discharger-attenuator behind the shaper output compressed the output pulses, 100-1000 MW pulses then being recorded on an S7-19 high-speed oscillograph. In the experiment with two pulse shaper-compressor stages a magnetron oscillator applied 500 kW f_3-pulses of 3.5 μs duration to the first stage (twin-T), from the output of which 15 MW f_3-pulses of 30 ns duration proceeded to the second stage (coaxial-T). In this experiment the oscillograph recorded 250 MW pulses of duration equal to 1.5 times the high-frequency duty cycle period. Adequate electric strength of the apparatus was ensured by holding the first pulse shaper in nitrogen under 0.015 MPa pressure and the second pulse shaper in nitrogen under 1 MPa pressure. Figures 2; references 8.

Effect of Flicker Noise on Korteweg-de Vries Equation Soliton

927J0077A Leningrad ZHURNAL TEKHNICHESKOY FIZIKI in Russian Vol 61 No 4, Apr 91 pp 186-190

[Article by V. M. Logvinov, Tuva Integrated Department at the Siberian Branch of the USSR Academy of Sciences, Kyzyl]

[Abstract] The appearance of flicker noise in materials of diverse origins, its diverse manifestations and physical mechanisms, and practical requirements of developing low-noise devices in today's microelectronics are discussed. The transformation of the Korteweg-de Vries (KDF) equation soliton in the Gaussian flicker noise field is investigated. The resulting data characterize the Korteweg-de Vries equation soliton evolution in the field of Gaussian flicker noise and demonstrate that Gaussian noise statistics are rather typical. The type of the noise statistics depends on the origin of the material in which noise is generated. It is noted that the soliton dynamics described by the Korteweg-de Vries equation may be simulated with the help of a nonlinear transmission line with dispersion; such a line, as a rule, represents a network of nonlinear links whose elements are diodes with variable capacitance or inductance and saturable ferromagnetic cores. Thus, a random force affecting the Korteweg-de Vries equation soliton may be defined as a random electromotive force (EMF) on the network input. References 8: 6 Russian, 2 Western.

Thermodynamical Validation of Least-Action Principle

927J0074A Tomsk IZVESTIYA VYSSHIKH UCHEBNYKH ZAVEDENIY: FIZIKA in Russian Vol 34 No 5, May 91 pp 53-59

[Article by V. N. Maslov, Moscow Institute of Chemical Apparatus Construction]

UDC 536.7

[Abstract] Extension of the least-action principle to nonequilibrium thermodynamics is considered, one difficulty in validation of this principle being that the state variables of equilibrium thermodynamics do not explicitly depend on their time derivatives and another difficulty involving existence of a solution to the variational problem. The possibility of a phenomenological validation of this principle for a large class of thermodynamic systems covering a wide range of the degree of nonequilibrium is demonstrated on a system which satisfies the criterion of thermal isolation, this criterion being no energy and mass exchange with other systems, and the volume of which cannot expand infinitely. The system consists of two separate subsystems, dissipation taking place in the closed one with any degree of nonequilibrium and energy exchange between the two assumed to be possible but thermodynamically reversible. A spontaneous Vlasov process, namely an inertial process not requiring participation of external forces, is assumed to take place in the dissipative subsystem. Such a process will, within a finite time, bring this subsystem and the system as a whole to the one only possible state of stable equilibrium (first law of thermodynamics) so that the system will have lost its capacity for work. The action of external forces during an inertial spontaneous process in a closed system is formulated in terms of the variational principle, with a zero first variation of their work. The second variation of their work is positive, inasmuch as these forces do work while the work capacity of the expanding isolated system decreases and thus virtual deviations from the real trajectory of the process are possible. The work capacity A of an isolated system is maximum and the energy dissipation ψ is consequently minimum along the real trajectory of an inertial spontaneous process, when compared with those along any other possible trajectory of an irreversible process: $\max A_p = A_s$ and $\min\psi = \psi_s$ (p - virtually possible, s - spontaneous) so that $\psi_s + A_s = \lim_{\psi\to 0} A_s = A_{max}$. Accordingly $\psi_s = (A_{max} - A_s > 0)$ (second law of thermodynamics) derives from the variational principle $\delta\psi = \delta(A_{max} - A_p) = 0$ and $\delta^2\psi > 0$. For a validation of the least-action principle, letting $\psi_s = -\Phi$ and $A_s = A$ transforms the equation $\Psi_s + A_s = A_{max}$ into $\Delta\Phi = A_{max} - A$ in integral form or $-\delta\Phi = dA_{max} - dA$ in differential form. The change of thermodynamic potential $\Delta\Phi$ as the system relaxes from initial nonequilibrium to equilibrium is then averaged over the thermodynamic time $\tau = +/-(t_e - t)$ ($0 \leq \tau < +\infty$, t_e - time to reach equilibrium): $(k/\Delta\Phi)\mathrm{Int}_0^{\tau 1} 2(-\Delta\Phi)\delta\tau$ (k - proportionality factor which is a constant when Φ and τ are the only independent variables, $\Delta\Phi = \tau 1$ 0). The variational principle corresponding to the equality $-\Delta\Phi = \min\psi$ is then $I = \mathrm{Int}_0^{\tau 1}\Phi\,\delta\tau = \min$. The thermodynamic potential is subsequently represented as Maslov's eigenfunction of a nonequilibrium system $\Phi = [\Phi^n$ to power n + 1]/(n + 1)Φ^n to power n with $\Phi^{n+1} = \mathrm{const}$ (n = 1,2,3,... denoting the eigenvalues of a parameter called the dissipative order of a process). Entropy has not been involved here so as not to limit the scope of the least-action principle to systems near equilibrium. On the other hand, inertia is not a universal property and there are non-Vlasov spontaneous processes such as certain life processes. The variational equation $\delta I = \delta.\mathrm{Int}_0^{\tau 1}\psi.\delta\tau = 0$, moreover, has also the solution $I = \mathrm{Int}_0^{\tau 1}\Delta\Phi\delta t = \max$ representing the maximum dissipation principle. Figures 2; references 15.

Nonequilibrium Thermo-Field Dynamics and Nonequilibrium Statistical Operator Method. I. General Relations

927J0086A Moscow TEORETICHESKAYA I MATEMATICHESKAYA FIZIKA in Russian Vol 88 No 2, Aug 91 pp 286-310

[Article by D. N. Zubarev, M. V. Tokaruk, Mathematics Institute imeni V. A. Steklov at the USSR Academy of Sciences, Condensed Media Physics Institute at the Ukrainian Academy of Sciences]

[Abstract] The development of the theory of nonequilibrium processes in quantum-field systems and formulations of nonequilibrium thermo-field dynamics are discussed; an attempt is made to formulate nonequilibrium thermo-field dynamics on the basis of the method of nonequilibrium statistical operator which realizes the concepts of abbreviated description of the nonequilibrium state in a general form. To this end, the nonequilibrium quantum statistical mechanics are reformulated in terms of superoperators of Liouville's thermal space on the basis of the method of nonequilibrium statistical operator; in addition, a general solution of Schroedinger's equation for a nonequilibrium thermo-vacuum state vector which depends on time only through the values of a certain set of observed variables is derived, thus solving the problem of plotting a quasiequilibrium thermo-vacuum, state vector as the initial state for solving Schroedinger's equation for the nonequilibrium thermo-vacuum state vector. Subsequently, general transport equations are derived for the mean values of abbreviation description variables and kinetic and hydrodynamic limiting cases are considered. A nonequilibrium thermo-vacuum state vector for quantum-field systems is found. The proposed approach may be used for describing relaxation processes in laser systems. The authors are grateful to I. R. Yukhnovskiy, Yu. L. Klimontovich, Yu. A. Tserkovnikov, V. G. Morozov, and G. O. Balabanyan for useful discussions and constructive criticism. References 63: 32 Russian, 31 Western.

Envelope Breezers and Solitons in Domain Wall of Uniaxial Ferromagnetic Material

927J0070A Moscow PISMA V ZHURNAL EKSPERIMENTALNOY I TEORETICHESKOY FIZIKI in Russian Vol 54 No 2, 25 Jul 91 pp 97-99

[Article by A. F. Popkov, Scientific Research Institute of Problems in Physics imeni F. V. Lukin, Moscow]

[Abstract] Breezers and solitons of the spin waves envelope localized in the domain walls of a ferromagnetic material are obtained theoretically by reduction of the equations of small-amplitude perturbations to a nonlinear Schroedinger equation of diffusion with additional perturbation terms which account for pumping and dissipation, also with corrections relating to space and time derivatives of "slow" variables. A ferromagnetic material with a high degree of uniaxial anisotropy is considered, for specificity, spin wave processes in its domain walls being adequately described by the system of Slonchevskiy equations in q (coordinate of shifting domain wall center along Y-axis) and ψ (azimuth angle of magnetization deflection from plane of domain wall which is parallel to XZ plane) with two parameters: Gilbert's attenuation constant α and coefficient b which represents the pinning force on domain wall in $q = 0$ plane. The solution to these equations is sought in the form of a double harmonic series, assuming a $\psi_0/q_0 = a[\rightarrow$ over $a] = 0$ vector for the unexcited ground state of a domain wall and a small oscillation amplitude in a nonlinear wave so that $|\psi| << \pi$. Exclusion of secular terms yields the evolution equation for the amplitude of the first harmonic. This nonlinear Schroedinger equation has soliton solutions which describe spin wave packets localized in a domain wall. In the approximation of very small wave vectors $k << b$, moreover, the single-soliton solutions describe standing wave packets of the breezer kind, these being of particular interest on account of their direct involvement in generation and annihilation of Bloch lines. The conditions for their existence in an alternating magnetic field are established in accordance with the perturbation theory for nonlinear Schroedinger solitons. Numerical estimates made for rare-earth ferrite-garnet films with Bloch lines indicate that the breezers can exist in these films. The author thanks V. M. Yeleonskiy, V. M. Zvezdin, and M. V. Chetkin for helpful discussion. References 11.

On Possibility of Splitting Ball Lightning Into Two

927J0077B Leningrad ZHURNAL TEKHNICHESKOY FIZIKI in Russian Vol 61 No 4, Apr 91 pp 25-31

[Article by A. I. Grigoryev, S. O. Shiryayeva, I. D. Grigoryeva, A. E. Lazaryants, Ye. I. Mukhina, Yaroslavl State University]

[Abstract] Eyewitness reports of ball lightnings (ShM) splitting into two comparably sized ball lightnings under natural conditions are discussed and an attempt is made to ascertain the physical characteristics of the ball lightning matter at which it may split into two. The analysis is carried out in the framework of an idealized continuum assuming that the ball lightning matter's free surface is characterized by a certain value of surface tension and that the ball lightning has a nonequalized electric charge under whose destabilizing effect the splitting process may occur. It is demonstrated that given a surface distribution of the ball lightning's electric self-charge, it cannot split into two under the effect of an electrohydrodynamic instability but is capable of ejecting its matter in the form of jets. If, however, the ball lightning has a bulk charge distribution, the opposite obtains: The ball lightning cannot eject a jet, yet is capable of splitting into two. Since both types of reaction have been reported by eyewitnesses, the conclusion is drawn that the ball lightning matter has poor conduction; if this is true, the ball lightning at the initial stage of its existence will be capable of splitting and at the terminal stage—ejecting a jet. The conclusion about the ball lightning's possibility of splitting into two can be equally applied to charged liquid drop aerosols, individual drops, and clusters, provided that the concept of surface tension can be used for the latter two phases. Figures 5; references 14: 9 Russian, 5 Western.

Self-Sustained Wave Process in Phase Transition Dynamics of Protein Film

927J0077C Leningrad ZHURNAL TEKHNICHESKOY FIZIKI in Russian Vol 61 No 4, Apr 91 pp 62-71

[Article by Ye. G. Rapis, G. Yu. Gasanova, Turkmen Scientific Research Institute of Eye Disease, Ashkhabad]

[Abstract] The development of self-ordering and self-sustained wave processes in biological matter is discussed and the task of interpreting the morphogenesis kinetics in a protein film and establishing the cause of the experimentally observed ordered morphological structure pattern during the drying of such film is formulated. The genesis dynamics of an ordered morphological structure during the solidification of a protein drop is examined by means of dynamic microscopic analysis of photography at equal time interval. An egg white film placed on a glass slide at a 27°C temperature is thus studied. A geometrically ordered structure referred to as a "drying rosella" with a regular crack orientation and a wave process in each "block" displaying the properties of self-sustained waves is discovered, attesting to the fact that the protein phase transition from a liquid to a solid state occurs through a self-sustained wave process which largely determines the protein's "drying rosella" morphology. The results make it possible to unify the physical, chemical, and biological origins of self-ordering and suggest that the geometric similarity of blocks and centers and their symmetry in a drying protein film to cells and their nuclei in the living world is not accidental. Figures 9; references 15.

New Technique of 1/n Expansion

927J0067A Moscow ZHURNAL EKSPERIMENTALNOY I TEORETICHESKOY FIZIKI in Russian Vol 100 No 8, Aug 91 pp 415-421

[Article by S. S. Stepanov and R. S. Tutik, Dnepropetrovsk State University]

[Abstract] Bound fundamental and radially excited states in the discrete spectrum of the Schroedinger equation $-h^2U''(r)/2m + [V(r) + h^2l(l + 1)/2mr^2 - E]U(r) = 0$ (l - orbital moment, h - Planck's constant) are considered, analysis of these states by the conventional semiclassical method of 1/N expansion being based on classical motion of a particle at the bottom of the potential well formed by the effective potential $V_{eff} = V(r) + h^2l(l + 1)/2mr^2$ with quantum fluctuations and anharmonicity then also taken into account. There are two known equivalent techniques of forming this expansion, both involving transition to the classical mechanics limit. One technique is to let the dimensionality D of space tend to infinity ($D \rightarrow \infty$) and then, after expansion into a power series in the small parameter $1/(l + D/2)$ or $1/(l - a + D/2)$ (a - shift parameter which improves the convergence), recover the physical dimensionality of space by letting $D = 3$. The other technique is to let the orbital moment tend to infinity ($l \rightarrow \infty$) so that also the principal quantum number $n = n_r + l + 1 \rightarrow \infty$, where the radial quantum number n_r is constant, and then select 1/n as the small parameter. Another possible semiclassical technique of forming the 1/N expansion involves explicit use of the expansion $h^2l(l + 1) \equiv \Lambda^2 + h\Lambda\Lambda + h^2B$. The solution to the accordingly modified Schroedinger equation is then expanded not into a power series in $1/\Lambda$, with the appropriate selection of parameters A, B, and Λ, but into a power series in the Planck's constant. The algorithm of the logarithmic perturbation theory will reduce that Schroedinger equation to a Ricatti equation so that difficulties in the standard description of radial perturbations can be avoided by use of quantization conditions, asymptotic expansions of the function $C(r) = hU'(r)/U(r)$ and of the energy function E yielding a chain of recurrence formulas for calculation of the energy. In the classical limit ($h \rightarrow 0$) the zeroth approximation of energy is $E_0 = V(r_0 + \Lambda^2/2mr_0^2$, which corresponds to motion of a classical particle in a stable circular orbit. Anharmonicity is taken into account by shifting the origin of coordinates to the r_0 point and expanding the effective potential into a Taylor series in $x = (r - r_0)/r_0$. This technique, which thus requires that the rule of transition to the classical limit be $h \rightarrow 0$ and $n_r = \text{const}$, complements the Wentzel-Kramers-Brillouin approximation method. It does, moreover, facilitate evaluation of the coefficients in terms of the 1/N expansion up to an arbitrarily high order. As an example is considered such a 1/n expansion of eigenvalues of the Schroedinger equation for a funnel-form potential $V(r) = -\kappa/r + r/a^2$. The authors thank G. M. Zinovyev for interest and helpful discussions. Tables 1; references 25.

Cycle Surfaces Method for Searching for Periodic Motions of Certain Variable-Structure Systems

927J0084A Kiev PRIKLADNAYA MEKHANIKA in Russian Vol 27 No 9, Sep 91 pp 114-119

[Article by Yu. Ya. Dusavitskiy, Moscow]

UDC 717.925.12

[Abstract] The need to examine differential equations with discontinuous right sides for developing automatic control systems, including switchable electronic systems, and the problems of determining the parameters of periodic solutions or the necessary switching conditions for ensuring given variables of periodic motion are addressed. A method of solving such problems in order to identify a system under study by its self-sustained oscillation parameters is considered. To this end, a method of searching for periodic motions of an off-line system described by changeable linear differential equations where the equation change procedure is determined by the switching conditions, which may be defined graphically, is examined. The examples of surface cycles for zero velocity error and zero position error systems are cited; in these systems the parameters are computed numerically. The surface cycles method's shortcoming is the need to completely recalculate and plot the entire set of surfaces when the parameters of the system under study change. The need for a mathematical description of isochrones and for determining the domains and conditions of surface cycles, stability conditions of the periodic solutions, and the dependence of periodic solution parameters on matrix coefficients is identified. The author is grateful to A. F. Filippov of the Moscow State University for help. Figures 3; references 4.

Foreign Broadcast Information Service (FBIS) and Joint Publications Research Service (JPRS) publications contain political, military, economic, environmental, and sociological news, commentary, and other information, as well as scientific and technical data and reports. All information has been obtained from foreign radio and television broadcasts, news agency transmissions, newspapers, books, and periodicals. Items generally are processed from the first or best available sources. It should not be inferred that they have been disseminated only in the medium, in the language, or to the area indicated. Items from foreign language sources are translated; those from English-language sources are transcribed. Except for excluding certain diacritics, FBIS renders personal names and place-names in accordance with the romanization systems approved for U.S. Government publications by the U.S. Board of Geographic Names.

Headlines, editorial reports, and material enclosed in brackets [ ] are supplied by FBIS/JPRS. Processing indicators such as [Text] or [Excerpts] in the first line of each item indicate how the information was processed from the original. Unfamiliar names rendered phonetically are enclosed in parentheses. Words or names preceded by a question mark and enclosed in parentheses were not clear from the original source but have been supplied as appropriate to the context. Other unattributed parenthetical notes within the body of an item originate with the source. Times within items are as given by the source. Passages in boldface or italics are as published.

SUBSCRIPTION/PROCUREMENT INFORMATION

The FBIS DAILY REPORT contains current news and information and is published Monday through Friday in eight volumes: China, East Europe, Central Eurasia, East Asia, Near East & South Asia, Sub-Saharan Africa, Latin America, and West Europe. Supplements to the DAILY REPORTs may also be available periodically and will be distributed to regular DAILY REPORT subscribers. JPRS publications, which include approximately 50 regional, worldwide, and topical reports, generally contain less time-sensitive information and are published periodically.

Current DAILY REPORTs and JPRS publications are listed in *Government Reports Announcements* issued semimonthly by the National Technical Information Service (NTIS), 5285 Port Royal Road, Springfield, Virginia 22161 and the *Monthly Catalog of U.S. Government Publications* issued by the Superintendent of Documents, U.S. Government Printing Office, Washington, D.C. 20402.

The public may subscribe to either hardcover or microfiche versions of the DAILY REPORTs and JPRS publications through NTIS at the above address or by calling (703) 487-4630. Subscription rates will be provided by NTIS upon request. Subscriptions are available outside the United States from NTIS or appointed foreign dealers. New subscribers should expect a 30-day delay in receipt of the first issue.

U.S. Government offices may obtain subscriptions to the DAILY REPORTs or JPRS publications (hardcover or microfiche) at no charge through their sponsoring organizations. For additional information or assistance, call FBIS, (202) 338-6735,or write to P.O. Box 2604, Washington, D.C. 20013. Department of Defense consumers are required to submit requests through appropriate command validation channels to DIA, RTS-2C, Washington, D.C. 20301. (Telephone: (202) 373-3771, Autovon: 243-3771.)

Back issues or single copies of the DAILY REPORTs and JPRS publications are not available. Both the DAILY REPORTs and the JPRS publications are on file for public reference at the Library of Congress and at many Federal Depository Libraries. Reference copies may also be seen at many public and university libraries throughout the United States.